Fig. (1). *Parg* gene-disruption in mouse ES cells. **A.** Gene-targeting strategy. The top lines represent the approximately 18 kb *Parg* genomic locus. The 3'-and 5'-recombination junction probes (3'-probe and 5'-probe, respectively) used to detect the disrupted alleles are shown as solid bars. The locations of restriction enzymes are also shown (N, *Nar*I; E, *Eco*RV; P, *Pst*I; X, *Xho*I; S, *Sac*I, B, *Bam*HI). The middle lines represent the targeting constructs and the positions of the selection marker genes. The sequence of *loxP* is depicted as slashed boxes. Linearization of *puro*^{r} vector with *Sac*I digestion resulted in separation of the *DT-A* cassette from the *Parg* gene sequence, however, *Parg*$^{-/-}$ ES cell clones were obtained at an expected frequency. **B.** Southern blot analysis of *Parg*$^{+/+}$, *Parg*$^{+/-}$ and two *Parg*$^{-/-}$ ES cell clones, D79 and D122. Hybridization with the 3'-probe was performed after digestion of genomic DNAs with *Bam*HI. Gene-disruption was also confirmed by Southern blot analysis using 5'-probe (data not shown).

TAATAC-3' and 5'-ATACAGTGCATAGAGACTGG-3'. PCR products were separated by electrophoresis and visualized by staining with ethidium bromide.

Poly(ADP-Ribose) Degradation and Parg Activity Measurement

ES cell lysate was prepared by suspending cells in a lysis buffer consisting of 20 mM potassium phosphate (pH 7.5), 2 mM EDTA, 10 mM β-mercaptoethanol, 0.1% Triton X-100 containing protease inhibitor cocktail (Complete™, Roche Diagnostics) and mixed in a blender at 4 °C for 30 min. After centrifugation at 18,000g at 4 °C for 15 min, the supernatant was taken and protein quantification was carried out. ^{32}P-Poly(ADP-ribose) was prepared using crude extract from *E. coli* overexpressing human PARP-1, as described [20, 21]. ^{32}P-Poly(ADP-ribose) was detached from the protein and further purified using anionic-exchange column chromatography. ^{32}P-Poly(ADP-ribose) was added at 5 μM (calculated as the ADP-ribose concentration) to the reaction mixture containing 20 mM potassium phosphate (pH 7.5), 2 mM EDTA, 10 mM β-mercaptoethanol, 0.1% Triton X-100, and the crude extracts of ES cells, incubated at 25 °C for 10 min. The aliquot was also used to measure the degradation activity of ^{32}P-poly(ADP-ribose) into ^{32}P-(ADP-ribose) by polyethyleneimine-impregnated cellulose TLC (thin-layer chromatography) plate (Macherey-Nagel) using a developing solvent consisting 3 M acetic acid, 0.1M LiCl and 3 M Urea, as described [20] and the TLC plates were analyzed by

BAS2500 (Fuji Film) and the radioactivity of degradation products and the remaining poly(ADP-ribose) was quantified.

Clonogenic Survival Assay

Clonogenic survival assay of ES cells were carried out as described [22, 23]. ES cells were inoculated in triplicate onto 6-well plates (Iwaki) with a STO cell feeder layer as described earlier. Cells were exposed to dimethyl sulfate (DMS, Sigma), cisplatin (Sigma), and hydrogen peroxide (Mitsubishi-Gas Chemicals), gemcitabine (Sigma), camptothecin (Sigma), and 5-fluorouracil (Sigma) at various concentrations for 16 hrs, rinsed two times in PBS and allowed to grow for 8 days. The numbers of ES cells inoculated per well were adjusted to yield at least several colonies on each plate, respectively, and ranged from 500 to 5 x 10^5 cells depending on the chemicals and their concentration or irradiation dose [24]. For γ-irradiation, trypsinized cells were irradiated using a ^{60}Co γ-irradiator at 0.29 Gy/sec, inoculated on a STO cell feeder layer and were left to grow for 8 days as above. The colonies were stained with crystal violet for counting. The clonogenic survival ratio to the untreated control was calculated as follows.

Plating efficiency (P. E.)= (No. of colonies)/(number of inoculated cells)

The clonogenic survival ratio to the untreated control= (P. E. at a given concentration of chemical or irradiation dose)/ (P. E. of untreated cells).

Western Blot Analysis

After sonication and separation by SDS-polyacrylamide gel electrophoresis, proteins were transferred onto Immobilon membranes (Millipore), the membrane was incubated with anti-α-tubulin (1:1,000, ICN Biomedicals), immune complexes were visualized using a horseradish peroxidase-linked secondary antibody and the enhanced chemiluminescence reaction (ECL Plus kit, Amersham). Detection of Timm23 protein was carried out using a monoclonal antibody against Timm23 (BD Bioscience Clontech) diluted at 1:2,500 as above. For detection of Parg, the anti-Parg mouse monoclonal antibody raised against a peptide from the C-terminal half of Parg and horseradish peroxidase-conjugated anti-mouse IgG were diluted with an immunoreaction enhancer solution, Can Get Signal^{TM} (TOYOBO), and incubated with an anti-Parg monoclonal antibody (1:250) for 1 hr and horseradish peroxidase-conjugated anti-mouse IgG (1:5,000) for 1 hr.

Statistical Analysis

Statistical analysis was carried out by Mann-Whitney U tests using SPSS software (Macintosh version, SPSS, Chicago) or JMP 5.1.2 (SAS Institute, Cary).

RESULTS

Generation of *Parg*$^{-/-}$ ES Cell Lines Lacking a Full Length Isoform

The *loxP/lacZ/neo*^{r} targeting vector allowed in-frame fusion of the *Parg* gene with *lacZ* at 47 bases downstream of the translation-initiation site in exon 1, and the insertion of the *loxP*-franked *neo*^{r} cassette downstream of the *lacZ* gene in the same orientation to *Parg* transcription, as shown in Fig. (1A). After electroporation into J1 ES cells, G418-resistant colonies were isolated and 4 of 704 clones were identified as *Parg*$^{+/-}$ ES cell clones by Southern blot analysis Fig. (1B). Disruption of the remaining allele with the *puro*^{r} targeting vector was performed on clone B609, and 6 of 230 *neo*^{r} and *puro*^{r} clones were identified to be *Parg*$^{-/-}$. Representative results of Southern blot analysis are presented as Fig. (1B). Two *Parg*$^{-/-}$ ES cell clones, D79 and D122, were employed for further analyses.

Northern blot analysis revealed that the amount of 4 kb *Parg* mRNA in *Parg*$^{-/-}$ ES cells was reduced approximately to one-sixth of that in *Parg*$^{+/+}$ ES cells (Fig. 2A). Cortes et al. reported that besides a full length *Parg* mRNA (variant 1) containing exons 1a, 1 and 2, a splice variant (variant 2), which lacks exon 1 but harbors exons 1a and 2, is present [11]. RT-PCR analysis using three primer sets specific for *Parg* mRNA (Fig. 2B) suggested that residual Parg transcripts present in *Parg*$^{-/-}$ ES cells correspond to variant 2 or truncated *Parg* mRNA possessing a second ATG colon present in exon 2. As shown in Fig. (2C) (marked with asterisk), western blot analysis revealed that the largest Parg isoform of around 128 kDa, which may correspond to the full length form, was lost in *Parg*$^{-/-}$ ES cell lines and the amounts of the two major isoforms of around 107 kDa and 63 kDa (marked with arrows) in *Parg*$^{-/-}$ ES cell clones were reduced. Al-

though other minor isoforms of 86, 78 and 59 kDa were not observed in *Parg*$^{-/-}$ ES cell clones by western blot analysis, we could not conclude whether these 86, 78 and 59 kDa minor isoforms were absent or present at reduced amounts in *Parg*$^{-/-}$ ES cell clones. The degradation activity of ^{32}P-poly(ADP-ribose) in ES cell extracts was reduced approximately to one-tenth in *Parg*$^{-/-}$ ES cell clones compared with *Parg*$^{+/+}$ ES cell clones (Fig. 2D and 2E). A major degradation product was ADP-ribose for both *Parg*$^{+/+}$ and *Parg*$^{-/-}$ ES cells, indicating that degradation to ADP-ribose by Parg is the main degradation pathway in ES cells.

The *Parg* gene shares a putative promoter with the *Timm23* gene [25]. RT-PCR analysis showed that *Timm23* expression level in *Parg*$^{-/-}$ ES cells did not change compared to *Parg*$^{+/+}$ ES cells (Fig. 2F). Western blot analysis showed that the amount of Timm23 protein in *Parg*$^{-/-}$ ES cells is comparable to that of the *Parg*$^{+/+}$ ES cells (Fig. 2G). Expression of fused *lacZ* mRNA driven from the *Parg* promoter in a *neo*^{r} allele was detected in *Parg*$^{-/-}$ ES cell clones by RT-PCR analysis (data not shown).

To confirm that the gene-targeting did not introduce additional sequence alterations in the *Parg* and *Timm23* genes of *Parg*$^{-/-}$ ES cell clones, we sequenced about 300 bp encompassing a 5'-junctional site of gene-targeting, in the *neo*^{r} and the *puro*^{r} allele, respectively, and found no sequence alteration in *Parg*$^{-/-}$ ES cell clones. We also sequenced approximately 500 bp of the *neo*^{r} allele, spanning a part of intron 1 and exon 1 of the *Timm 23*, *Timm23/Parg* promoter and *Parg* exon 1. The approximately 480 bp region of the *puro*^{r} allele, spanning the *Timm23 exon 1*, *Parg/Timm23* promoter, *Parg* exon 1 and the *puro*^{r} promoter was sequenced as well. Two serial gene-targeting events were suggested to produce the targeted alleles precisely and additional mutations were not found at the 5'-junctional site of gene-targeting in *Parg*$^{-/-}$ ES cell clones D79 and D122.

These results indicate that targeted disruption of *Parg* gene exon 1 eliminated the transcript, which encodes a full-length isoform of Parg, and also caused a marked reduction in the amount of other Parg transcripts encoding putative Parg isoforms.

In Vitro Growth of ES Cell Clones

Growth-rates of two *Parg*$^{-/-}$ ES cell clones, in the absence of a STO cell feeder layer were similar to those for parental J1 and *Parg*$^{+/-}$ ES cell clones. Doubling-time was calculated to be about 9 h in all cases and statistical differences in growth were not observed among the genotypes (Fig. 3A). No proliferation impediment was observed in at least 50 successive passages in the absence of the feeder layer in each genotype.

Sensitivity of *Parg*$^{-/-}$ ES Cell Clones to DNA Damaging Agents of Various Types

Clonogenic survival assays revealed that *Parg*$^{-/-}$ ES cell clones show about 1.5-fold increased lethality with the monofunctional alkylating agent, DMS compared to their *Parg*$^{+/+}$ counterpart, as illustrated in Fig. (3B) ($p<0.05$). *Parp-1*$^{-/-}$ ES cell clone exhibited increased lethality only at
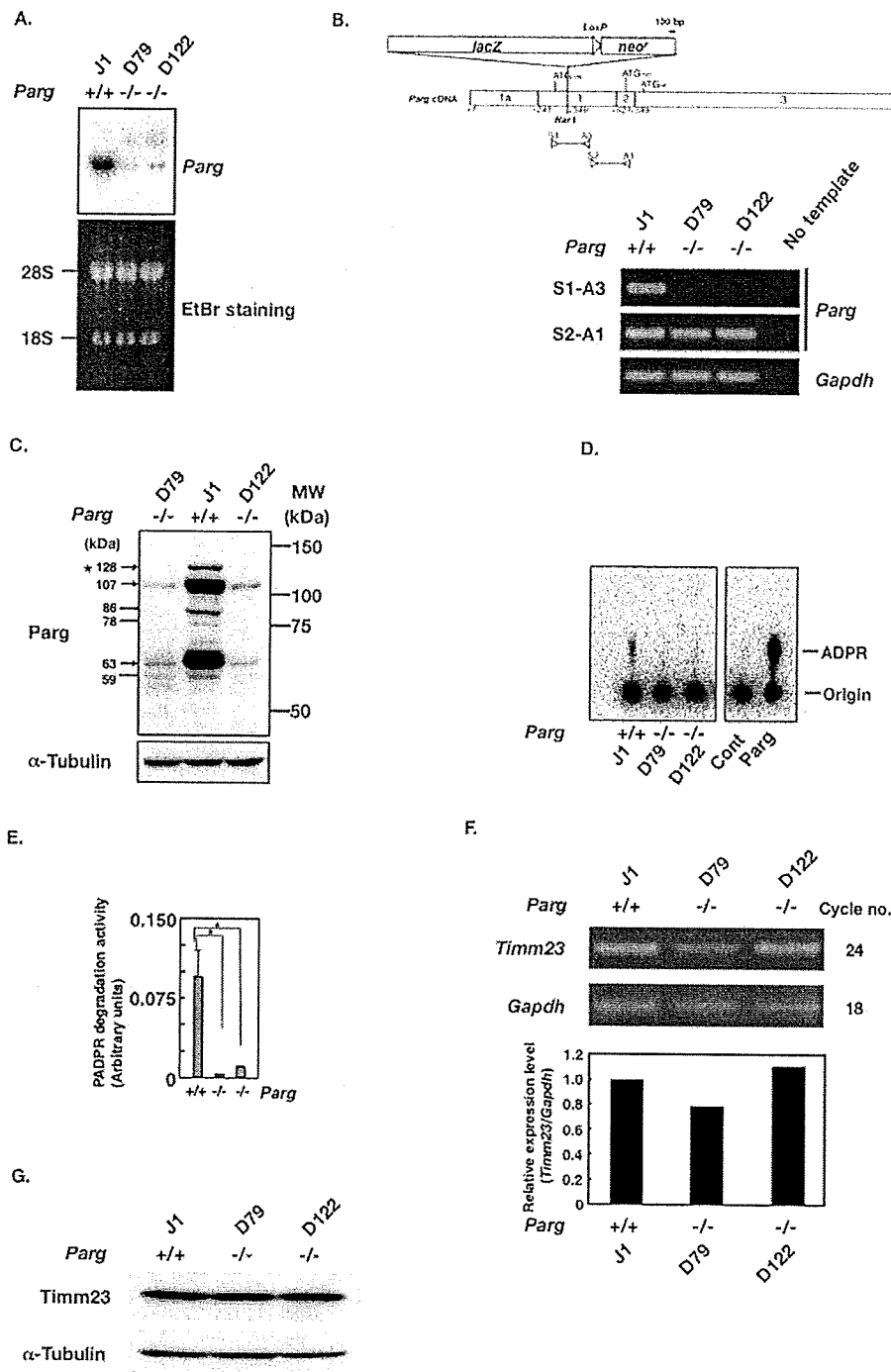
Fig. (2). A. Northern blot analysis. Thirty μg of total RNA isolated from ES cells was analyzed by Northern blot analysis using the *Parg* cDNA probe. **B.** Upper panel: Structure of the reported *Parg* cDNA in *Parg*^{-/-} ES cell clones. The positions of primer set, S1 and A3, spanning the targeting site and another PCR set, S2 and A1, located downstream of the targeting site are shown. Lower panel: Total RNA isolated from ES cells was used to generate cDNAs and the PCR reaction was carried out using primer sets S1-S3 and S2-S1. **C.** Western blot analysis of Parg protein in ES cells. Total lysate of ES cells was subjected to western blot analysis using a monoclonal antibody against Parg and antibodies against α-tubulin. Arrows show major Parg isoforms and asterisks show minor Parg isoforms in *Parg*^{+/+} ES cells. **D & E.** The measurement of poly(ADP-ribose) degradation activity in the crude extracts of ES cell clones by TLC. A representative result of the TLC (**D**). Cont, control. The quantification graph (**E**). Bar, mean ± SE. **F.** RT-PCR analysis of the *Timm23* gene. The length of the PCR product was 220 bp as expected. **G.** Western blot analysis of Timm23 in *Parg*^{-/-} ES cells. Western blot analysis was carried out using a monoclonal antibody against Timm23 diluted at 1:2,500.
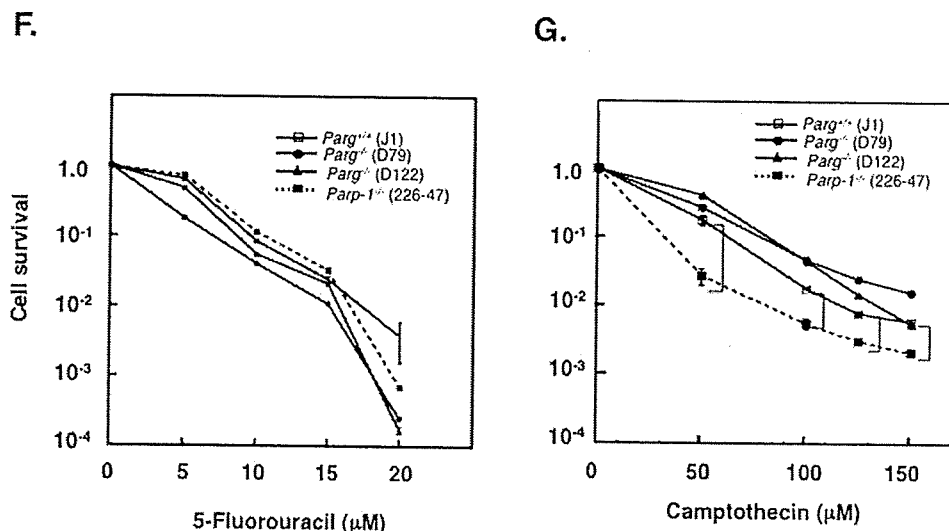
A.

B.

C.

D.

E.

F.

G.
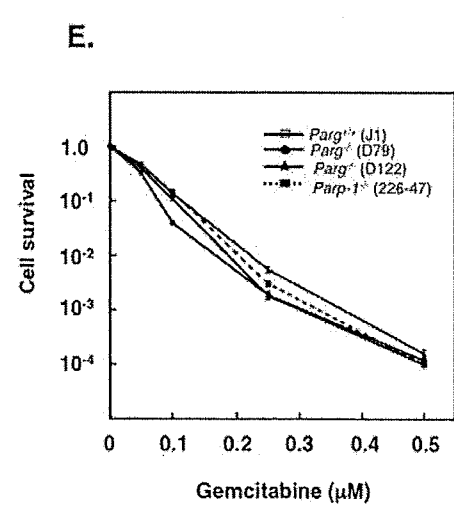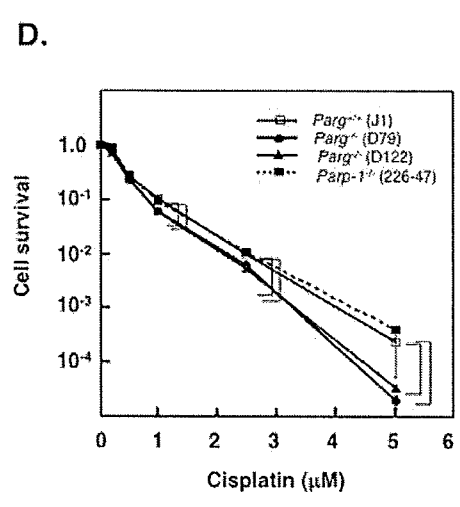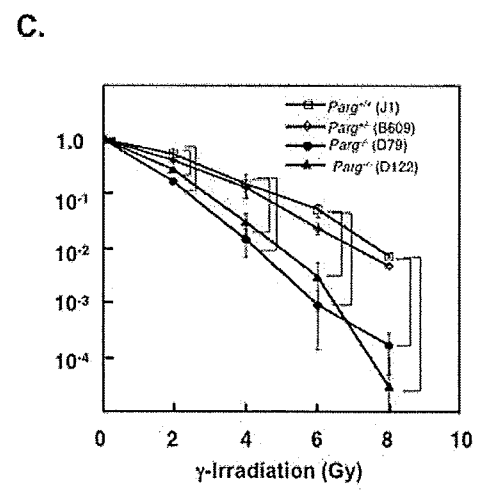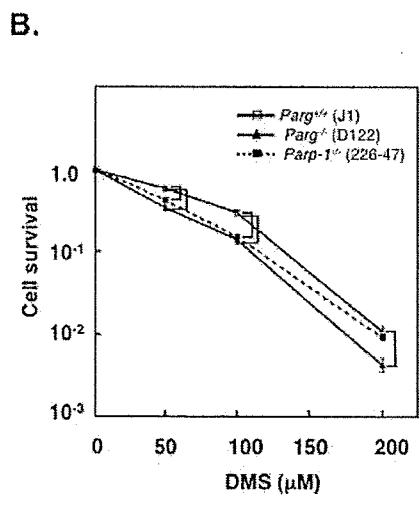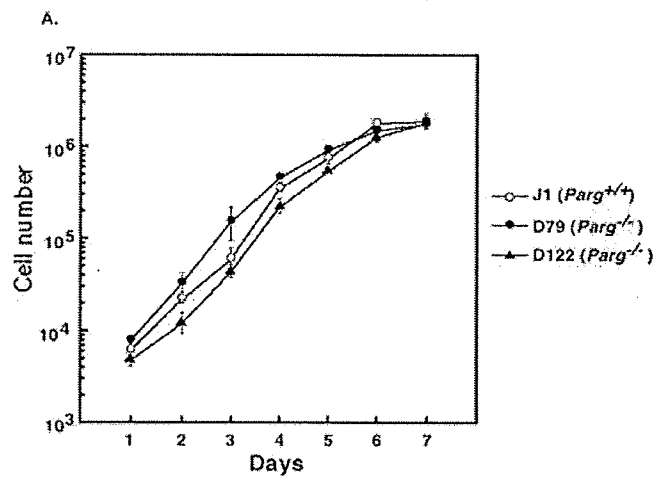
Fig. (3). Growth of ES cells and their survival after treatment with DNA damaging agents and γ-irradiation. A. Growth curves of ES cell clones *in vitro*. Growth of *Parg*$^{+/+}$, *Parg*$^{+/-}$ and two *Parg*$^{-/-}$ ES cell clones, D79 and D122, was measured in the absence of a STO feeder layer. All the samples were analyzed in triplicate. Bars, SE. The statistical significance was not observed at continuous four time points with *Parg*$^{+/-}$ or *Parg*$^{-/-}$ ES cell clones when compared to between *Parg*$^{+/+}$ ES cell clone. B-E. Survival curves of wild-type, *Parg*$^{-/-}$ and *Parp-1*$^{-/-}$ ES cell clones after treatment with DNA damaging agents. DMS (B). *Parg*$^{-/-}$ ES cell clone D79 showed the same level of enhanced lethality compared to *Parg*$^{-/-}$ ES cell clone D122 (data not shown). Cisplatin (D), gemcitabine (E), 5-fluorouracil (F), camptothecin (G) and γ-irradiation (C). Clonogenic survival assays were performed in triplicate as described in EXPERIMENTAL PROCEDURES. Bars, SE. When the values of survival for *Parg*$^{-/-}$ or *Parp-1*$^{-/-}$ genotype consistently showed more than two-fold differences compared to wild-type ES cell clone, the significant differences (*p*<0.05) were indicated with brackets.

50-100 µM but not at 200 µM concentration of DMS (Fig. 3B). Similarly, γ-irradiation caused a 1.5-fold greater lethality (*p*<0.05) in *Parg*$^{-/-}$ ES cell clones compared to *Parg*$^{+/+}$ ES cell clones (Fig. 3C). We previously reported that *Parp-1*$^{-/-}$ ES cell clones showed the similar level of enhanced sensitivity to γ-irradiation [22]. *Parg*$^{-/-}$ ES cell clones also showed increased lethality against treatment with cisplatin as well (Fig. 3D), whereas *Parp-1*$^{-/-}$ ES cell clones did not (Fig. 3D). After treatment with gemcitabine, a fluorinated analog of deoxycytidine, cell survival was not different between *Parg*$^{-/-}$ and *Parg*$^{+/+}$ ES cell clones (Fig. 3E). No difference in the clonogenic survival was also observed with *Parp-1*$^{-/-}$ ES cells (Fig. 3E), either. After 5-fluorouracil treatment, *Parg*$^{-/-}$ ES cell clones showed increased lethality at 20 µM concentration (*p*<0.05) but not at lower concentrations like in the case with *Parp-1*$^{-/-}$ ES cell clones (Fig. 3F). No increase in lethality was observed with camptothecin in *Parg*$^{-/-}$ ES cell clones, and a tendency of slight resistance to camptothecin was noted (Fig. 3G). In contrast, *Parp-1*$^{-/-}$ ES cell clones show increased lethality to the treatment with camptothecin (Fig. 3G). Regarding sensitivity to hydrogen peroxide, there was no difference between the *Parg*$^{+/+}$ and *Parg*$^{-/-}$ genotypes (data not shown) like in the case between the wild-type and *Parp-1*$^{-/-}$ ES cell clones [24].

Time Course of Cell Death in *Parg*$^{-/-}$ ES Cell Clones After DMS Treatment

Apoptotic oligonucleosomal DNA ladder formation was observed in *Parg*$^{+/+}$ ES cells 24 hr after addition of 0.1 mM

DMS, whereas clear DNA ladder formation was observed already at 10 hr in *Parg*$^{-/-}$ ES cells (Fig. 4). The increased level of DNA ladder was also evident at 24 hrs in *Parg*$^{-/-}$ ES cells compared to *Parg*$^{+/+}$ ES cells. *Parp-1*$^{-/-}$ ES cell clones also exhibited enhancement of DNA ladder formation at 24 hr but not at 10 hr compared with wild-type ES cells. Therefore, there is a distinct difference in cell death process between *Parg*$^{-/-}$ and *Parp-1*$^{-/-}$ ES cells.

DISCUSSION

In the present study, we generated hypomorphic mutant ES cells of *Parg* by eliminating the *Parg* transcript encoding a full length isoform and by reducing other Parg isoforms, including a mitochondrial Parg isoform. Parg isoforms, including splicing variants are likely targeted to different subcellular regions [26-28]. Parg activity in *Parg*$^{-/-}$ ES cells was reduced to one-tenth of *Parg*$^{+/+}$ ES cells. We confirmed that our gene targeting method did not affect expression of the *Timm23* gene present at upstream region of the *Parg* gene. The protein level of Timm23 was not different between *Parg*$^{+/+}$ and *Parg*$^{-/-}$ ES cell clones. This suggests that the observed phenotypes in *Parg*$^{-/-}$ ES cells are caused by *Parg* gene disruption but not by *Timm23* gene disruption. *Parg*$^{-/-}$ ES cells showed no alteration in growth rate from *Parg*$^{+/+}$ ES cells (Fig. 3A), whereas *Parg*$^{-/-}$ trophoblast stem cells derived from embryos derived from *Parg* null mice disrupted at exon 4 were only viable when PARP activity was inhibited by PARP inhibitors [29]. This difference in the viability of
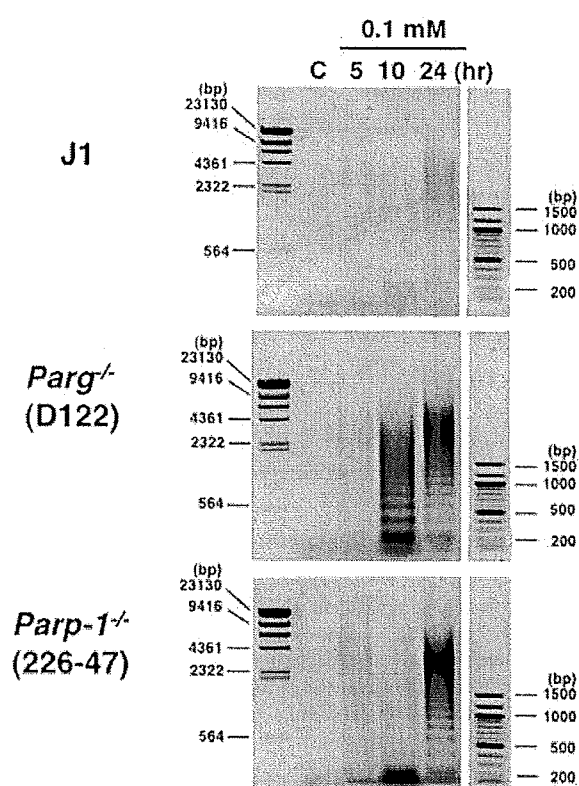
Fig. (4). Time course analysis of cell death after DMS treatment. Wild-type, *Parg*^{-/-} and *Parp-1*^{-/-} ES cell clones were cultured in the absence of a STO feeder layer and harvested, at each time point. Oligonucleosomal DNA ladder formation was analyzed by 2% agarose gel electrophoresis.

their and our *Parg* deficient cells is probably caused by the difference in the residual level of Parg activity. In the *Parg*^{-/-} ES cells, which we established, residual poly(ADP-ribose) degradation activity was 10% compared with wild-type ES cells, mainly covered by the isoforms of Parg (Fig. 2C, 2D, & 2E). The level of Parg activity seems to support the normal growth in the absence of cellular stress, although the difference in cell type, namely ES cells vs. trophoblast stem cells, may also affect the effect on growth.

We compared the effect of *Parg* deficiency on cytotoxicity of different types of DNA damaging agents using a clonogenic survival assay. *Parg*^{-/-} ES cell clones showed increased lethality against treatment with an alkylating agent, DMS, cisplatin and γ-irradiation. These results suggest that efficient poly(ADP-ribose) degradation by Parg is positively involved in cell recovery from DNA damage of particular types. After DMS treatment, *Parg*^{-/-} ES cell clones exhibited early and increased induction of apoptotic cell death. Our result support the notion that *Parg* deficiency results in increased cytotoxicity of alkylating agents and γ-irradiation [6,11,12]. On the other hand, there was no increase in sensitization against 5-fluorouracil at 15 μM or lower concentration for both *Parg*^{-/-} and *Parp-1*^{-/-} ES cell clones, although an increased sensitization against 5-fluorouracil was noted at 20

μM for both *Parg*^{-/-} and *Parp-1*^{-/-} ES cell clones. Regarding another nucleoside analog, gemcitabine, no sensitization effect in *Parg*^{-/-} or *Parp-1*^{-/-} ES cell clones was observed at the examined concentration range. 5-Fluorouracil inhibits thymidylate synthase and causes dTTP depletion, dNTP pool imbalance and apoptosis [30]. On the other hand, gemcitabine is known to cause inhibition of ribonucleotide reductase, dNTP depletion and replication stall or termination [30]. The results suggest that *Parg* and *Parp-1* deficiency do not critically affect cell death induced by these nucleoside analogs.

It is also notable that the sensitivity spectrum to DNA damaging agents in *Parg*-deficient ES cells partially but not completely overlaps that of *Parp-1* deficient ES cells. To the treatment with alkylating agents and γ-irradiation, *Parg* and *Parp-1* [22] deficiency both resulted in increased sensitivity. Against treatment with cisplatin, which mainly induces inter- or intra-strand DNA crosslinks, *Parg* deficiency leads to augmented sensitivity ($p<0.05$), whereas *Parp-1* deficiency does not in ES cells. Against treatment with camptothecin, *Parg* deficiency did not sensitize ES cells whereas *Parp-1* deficiency resulted in increased sensitivity.

Parg is suggested to be involved in single strand break repair [6, 31] and this may partially explain the enhanced lethality against alkylating agents and γ-irradiation under *Parg* deficiency. In contrast, the major repair pathways of DNA damage induced by cisplatin require nucleotide excision repair, mismatch repair and homologous recombination repair proteins [32]. The role of Parg in the repair pathway of DNA damage caused by cisplatin remains to be clarified. Parp-1 is shown to be involved in the repair of camptothecin-induced DNA damage, at reactivation process of the camptothecin-DNA-topoisomerase I cleavable complex [33], therefore increased lethality in *Parp-1*^{-/-} ES cells is consistent with this model. By contrast, the sensitization to camptothecin was not observed in *Parg*-deficient ES cells, suggesting that Parg may not be essentially involved in this repair process.

Enhancement of cytotoxicity of DNA damaging agents by *Parg* deficiency may also be partially explained by the involvement of Parg in the cell death regulation process. After treatment with DMS, we observed that apoptotic cell death pathway is augmented under *Parg* deficiency. It was previously demonstrated that apoptosis-inducing factor (AIF), a mitochondrial oxidoreductase, mediates Parp-1-dependent cell death accompanying NAD depletion [34]. Poly(ADP-ribose) was reported to induce cell death through induction of AIF release from mitochondria in the neuronal cells [35]. The data showing the classic apoptotic DNA laddering is accelerated after treatment with DMS in the *Parg*^{-/-} ES cells suggests that the AIF pathway may not predominate. *Parg*^{-/-} ES cells did not show increased sensitivity to hydrogen peroxide but do to γ-irradiation, although these two agents have many common aspects of their cytotoxicity. As we previously reported, *Parp-1*^{-/-} ES cells also showed increased sensitivity to γ-irradiation but not to hydrogen peroxide [24]. It could be speculated that cell-type dependent responses to different types of DNA damage might be present. In ES cells, cell death induction by hydrogen peroxide are not affected by *Parp-1* and *Parg* defi-

cienecy. Taken together, the results imply that functional inhibition of Parg leads to increased cytotoxicity of DNA damaging agents of some types.

The increases in cell killing by *Parg* deficiency is around1.5 fold in ES cells for DMS, γ-irradiation. For cisplatin and 5-fluorouracil, the increase less than 1.5 fold in sensitivity was observed. For treatment with the alkylating agent and γ-irradiation, *Parg*$^{-/-}$ ES cells and *Parp-1*$^{-/-}$ ES cells show comparable level of increase in sensitivity. Considering the fact that Parp inhibitors are being tested to sensitize the effect of alkylating agents and γ-irradiation in pre-clinical and clinical trials of cancer therapy [10, 36], it should be important to point out that the sensitizing effect against alkylating agents, cisplatin and γ-irradiation under *Parg* deficiency was observed, even it is apparently small in ES cells. Therefore, there is a possibility that Parg may become a novel sensitization target for chemotherapy with alkylating agent treatment or radiation therapy of cancer. The effect of *Parg* deficiency on sensitivity to DNA damaging agents should be examined in various types of cancer cells including those of human. Differences in cancer cell type should also affect the sensitization effect by *Parg* deficiency. Since ES cells retain stem cell properties, functional inhibition of Parg may be a strategy to target cancer stem population. Further studies are necessary to delineate the effect of *Parg*–deficiency in cell death induction mechanisms in cancer cells.

Inhibitors of Parg might be clinically useful in sensitizing cancer cells to certain types of chemotherapeutic agents that target DNA, including alkylating agents and cisplatin, and also to radiation therapy. Tentori et al. reported that an inhibitor of Parg, *N*-bis-(3-phenyl-propyl)9-oxo-fluorene-2, 7-diamide, sensitized malignant melanoma cells to the treatment of temozolomide [14]. Basic studies on optimization of treatment conditions for Parg inhibitors with combination of various types of DNA damaging agents are necessary. On the other hand, protection of Parg from its inactivation in normal cells is also of importance in diverse clinical situations to prevent apoptosis in healthy cell population.

The mechanism of sensitization to genotoxic agents by Parg functional inhibition should be further studied in different cell types and should be carried out carefully to explain distinct differences in the effect of *Parg* deficiency observed with the various DNA damaging agents. Only a limited number of Parg inhibitors have been reported [14, 21, 37-40], therefore, development of specific and effective Parg inhibitors should be also necessary.

ACKNOWLEDGMENTS

ABBREVIATIONS

AIF	=	apoptosis-inducing factor
ARH	=	ADP-ribose-(arginine) protein hydrolase
DMS	=	dimethyl sulfate
DT-A	=	diphtheria toxin A
ES cell	=	embryonic stem cell
lacZ	=	*β-galactosidase* gene
Parg	=	poly(ADP-ribose) glycohydrolase
Parp	=	poly(ADP-ribose) polymerase
PBS	=	phosphate-buffered saline
TLC	=	thin-layer chromatography

REFERENCES

[1]　Miwa, M.; Sugimura, T. Splitting of the ribose-ribose linkage of poly(adenosine diphosphate-ribose) by a calf thymus extract. *J. Biol. Chem.* 1971, *246*, 6362-6364.

[2]　Okayama, H.; Honda, M.; Hayaishi, O. Novel enzyme from rat liver that cleaves an ADP-ribosyl histone linkage. *Proc. Natl. Acad. Sci. USA* 1978, *75*, 2254-2257.

[3]　Oka, J.; Ueda, K.; Hayaishi, O.; Komura, H.; Nakanishi, K. ADP-ribosyl protein lyase. Purification, properties, and identification of the product. *J. Biol. Chem.* 1984, *259*, 986-995.

[4]　Oka, S.; J. Kato, J.; Moss, J. Identification and characterization of a mammalian 39-kDa poly(ADP-ribose) glycohydrolase. *J. Biol. Chem.* 2006, *281*, 705-713.

[5]　Maruta, H.; Matsumura, N.; Tanuma, S. Role of (ADP-ribose)n catabolism in DNA repair. *Biochem. Biophys. Res. Commun.* 1997, *236*, 265-269.

[6]　Fisher, A. E.; Hochegger, H.; Takeda, S.; Caldecott, K. W. Poly(ADP-ribose) polymerase 1 accelerates single-strand break repair in concert with poly(ADP-ribose) glycohydrolase. *Mol. Cell. Biol.* 2007, *27*, 5597-5605.

[7]　Durkacz, B. W.; Omidiji, O.; Gray, D. A.; Shall, S. (ADP-ribose)n participates in DNA excision repair. *Nature* 1980, *283*, 593-596.

[8]　Dantzer, F.; Schreiber, V.; Niedergang, C.; Trucco, C.; Flatter, E.; de La Rubia, G.; Oliver, J.; Rolji, V.; Menissier-De Murcia, J.; de Murcia, G. Involvement of poly(ADP-ribose) polymerase in base excision repair. *Biochimie* 1999, *81*, 69-75.

[9]　Plummer, E. R.; Middleton, M. R.; Jones, C.; Olsen, A.; Hickson, I.; McHugh, P.; Margison, G. P.; McGown, G.; Thorncroft, M.; Watson, A. J.; Boddy, A. V.; Calvert, A. H.; Harris, A. L.; Newell, D. R.; Curtin, N. J. Temozolomide pharmacodynamics in patients with metastatic melanoma: dna damage and activity of repair enzymes O6-alkylguanine alkyltransferase and poly(ADP-ribose) polymerase-1. *Clin. Cancer Res.* 2005, *11*, 3402-3409.

[10]　Zaremba, T.; Curtin, N. J. PARP inhibitor development for systemic cancer targeting. *Anticancer Agents Med. Chem.* 2007, *7*, 515-523.

[11]　Cortes, U.; Tong, W. M.; Coyle, D. L.; Meyer-Ficca, M. L.; Meyer, R. G.; Petrilli, V.; Herceg, Z.; Jacobson, E. L.; Jacobson, M. K.; Wang, Z. Q. Depletion of the 110-kilodalton isoform of poly(ADP-ribose) glycohydrolase increases sensitivity to genotoxic and endotoxic stress in mice. *Mol. Cell. Biol.* 2004, *24*, 7163-7178.

[12]　Koh, D. W.; Dawson, T. M.; Dawson, V. L. Mediation of cell death by poly(ADP-ribose) polymerase-1. *Pharmacol. Res.* 2005, *52*, 5-14.

[13]　Blenn, C.; Althaus, F. R.; Malanga, M. Poly(ADP-ribose) glycohydrolase silencing protects against H$_2$O$_2$-induced cell death. *Biochem. J.* 2006, *396*, 419-429.

[14]   Tentori, L.; Leonetti, C.; Scarsella, M.; Muzi, A.; Vergati, M.; Forini, O.; Lacal, P. M.; Ruffini, F.; Gold, B.; Li, W.; Zhang, J.; Graziani, G. Poly(ADP-ribose) glycohydrolase inhibitor as chemosensitiser of malignant melanoma for temozolomide. *Eur. J. Cancer* 2005, *41*, 2948-2957.

[15]   Ying, W.; Sevigny, M. B.; Chen, Y.; Swanson, R. A. Poly(ADP-ribose) glycohydrolase mediates oxidative and excitotoxic neuronal death. *Proc. Natl. Acad. Sci. USA* 2001, *98*, 12227-12232.

[16]   Formentini, L.; Arapistas, P.; Pittelli, M.; Jacomelli, M.; Pitozzi, V.; Menichetti, S.; Romani, A.; Giovannelli, L.; Moroni, F.; Chiarugi, A. Mono-galloyl glucose derivatives are potent poly(ADP-ribose) glycohydrolase (PARG) inhibitors and partially reduce PARP-1-dependent cell death. *Br. J. Pharmacol.* 2008, *155*, 1235-1249.

[17]   Mintz, B.; Illmensee, K. Normal genetically mosaic mice produced from malignant teratocarcinoma cells. *Proc. Natl. Acad. Sci. USA* 1975, *72*, 3585-3589.

[18]   Watanabe, S.; Kai, N.; Yasuda, M.; Kohmura, N.; Sanbo, M.; Mishina, M.; Yagi, T. Stable production of mutant mice from double gene converted ES cells with puromycin and neomycin. *Biochem. Biophys. Res. Commun.* 1995, *213*, 130-137.

[19]   Masutani, M.; Nozaki, T.; Nishiyama, E.; Ochiya, T.; Wakabayashi, K.; Suzuki, H.; Sugimura, T. Establishment of poly(ADP-ribose) polymerase-deficient mouse embryonic stem cell lines. *Proc. Jpn. Acad.* 1998, *74*(Ser. B), 233-236.

[20]   Shimokawa, T.; Masutani, M.; Nagasawa, S.; Nozaki, T.; Ikota, N.; Aoki, Y.; Nakagama, H.; Sugimura, T. Isolation and cloning of rat poly(ADP-ribose) glycohydrolase: presence of a potential nuclear export signal conserved in mammalian orthologs. *J. Biochem. (Tokyo)* 1999, *126*, 748-755.

[21]   Shirato, M.; Tozawa, S.; Maeda, D.; Watanabe, M.; Nakagama, H.; Masutani, M. Poly(etheno ADP-ribose) blocks poly(ADP-ribose) glycohydrolase activity. *Biochem. Biophys. Res. Commun.* 2007, *355*, 451-456.

[22]   Masutani, M.; Nozaki, T.; Nishiyama, E.; Shimokawa, T.; Tachi, Y.; Suzuki, H. ; Nakagama, H. ; Wakabayashi, K.; Sugimura, T. Function of poly(ADP-ribose) polymerase in response to DNA damage: gene-disruption study in mice. *Mol. Cell. Biochem.* 1999, *193*, 149-152.

[23]   Moynahan, M. E.; Cui, T. Y.; Jasin, M. Homology-directed dna repair, mitomycin-c resistance, and chromosome stability is restored with correction of a Brca1 mutation. *Cancer Res.* 2001, *61*, 4842-4850.

[24]   Ogino, H. ; Shibata, A.; Gunji, A.; Suzuki, H.; Nakagama, H.; Sugimura, T.; Masutani, M. Agent-dependent effects of Parp-1 deficiency on DNA damage responses and genomic stability in mouse ES cells. In: *New Developments in Stem Cell Research*; E. Grier Ed.; Nova Science Publishers, Inc.: Happauge, New York, USA, 2006, pp.133-147.

[25]   Meyer, R. G.; Meyer-Ficca, M. L.; Jacobson E. L.; Jacobson, M. K. Human poly(ADP-ribose) glycohydrolase (PARG) gene and the common promoter sequence it shares with inner mitochondrial membrane translocase 23 (TIM23). *Gene* 2003, *314*, 181-190.

[26]   Ohashi, S.; Kanai, M.; Hanai, S.; Uchiumi, F.; Maruta, H.; Tanuma, S.; Miwa, M. Subcellular localization of poly(ADP-ribose) glycohydrolase in mammalian cells. *Biochem. Biophys. Res. Commun.* 2003, *307*, 915-921.

[27]   Ame, J. C.; Jacobson E. L.; Jacobson, M. K. Molecular heterogeneity and regulation of poly(ADP-ribose) glycohydrolase. *Mol. Cell. Biochem.* 1999, *193*, 75-81.

[28]   Meyer-Ficca, M. L.; Meyer, R. G.; Coyle, D. L.; Jacobson, E. L.; Jacobson, M. K. Human poly(ADP-ribose) glycohydrolase is expressed in alternative splice variants yielding isoforms that localize to different cell compartments. *Exp. Cell Res.* 2004, *297*, 521-532.

[29]   Koh, D. W.; Lawler, A. M.; Poitras, M. F.; Sasaki, M.; Wattler, S.; Nehls, M. C.; Stoger, T.; Poirier, G. G.; Dawson, V. L.; Dawson, T. M. Failure to degrade poly(ADP-ribose) causes increased sensitivity to cytotoxicity and early embryonic lethality. *Proc. Natl. Acad. Sci. USA* 2004, *101*, 17699-17704.

[30]   Sampath, D.; Rao, V. A.; Plunkett, W. Mechanisms of apoptosis induction by nucleoside analogs. *Oncogene* 2003, *22*, 9063-9074.

[31]   Keil, C.; Grobe, T.; Oei, S. L. MNNG-induced cell death is controlled by interactions between PARP-1, poly(ADP-ribose) glycohydrolase, and XRCC1. *J. Biol. Chem.* 2006, *281*, 34394-34405.

[32]   Martin, L. P.; Hamilton, T. C.; Schilder, R. J. Platinum resistance: the role of DNA repair pathways. *Clin. Cancer Res.* 2008, *14*, 1291-1295.

[33]   Malanga, M.; Althaus, F. R. Poly(ADP-ribose) reactivates stalled DNA topoisomerase I and induces DNA strand break resealing. *J. Biol. Chem.* 2004, *279*, 5244-5248.

[34]   Yu, S. W.; Wang, H.; Poitras, M. F.; Coombs, C.; Bowers, W. J.; Federoff, H. J.; Poirier, G. G.; Dawson, T. M.; Dawson, V. L. Mediation of poly(ADP-ribose) polymerase-1-dependent cell death by apoptosis-inducing factor. *Science* 2002, *297*, 259-263.

[35]   Andrabi, S. A.; Kim, N. S.; Yu, S. W.; Wang, H.; Koh, D. W.; Sasaki, M.; Klaus, J. A.; Otsuka, T.; Zhang, Z.; Koehler, R. C.; Hurn, P. D.; Poirier, G. G.; Dawson V. L.; Dawson, T. M. Poly(ADP-ribose) (PAR) polymer is a death signal. *Proc. Natl. Acad. Sci. USA* 2006, *103*, 18308-18313.

[36]   Plummer, R.; Jones, C.; Middleton, M.; Wilson, R.; Evans, J.; Olsen, A.; Curtin, N.; Boddy, A.; McHugh, P.; Newell, D.; Harris, A.; Johnson, P.; Steinfeldt, H.; Dewji, R.; Wang, D.; Robson, L.; Calvert, H. Phase I study of the poly(ADP-ribose) polymerase inhibitor, AG014699, in combination with temozolomide in patients with advanced solid tumors. *Clin. Cancer Res.* 2008, *14*, 7917-7923.

[37]   Aoki, K.; Nishimura, K.; Abe, H.; Maruta, H.; Sakagami, H.; Hatano, T.; Okuda, T.; Yoshida, T.; Tsai, Y. J.; Uchiumi, F.; Tanuma, S. Novel inhibitors of poly(ADP-ribose) glycohydrolase. *Biochim. Biophys. Acta* 1993, *1158*, 251-256.

[38]   Slama, J. T.; Aboul-Ela, N.; Goli, D. M.; Cheesman, B. V.; Simmons, A. M.; Jacobson, M. K. Specific inhibition of poly(ADP-ribose) glycohydrolase by adenosine diphosphate (hydroxymethyl)pyrrolidinediol. *J. Med. Chem.* 1995, *38*, 389-393.

[39]   Masutani, M.; Shimokawa, T.; Igarashi, M.; Hamada, M.; Shibata, A.; Oami, S.; Nozaki, T.; Nakagama, H.; Sugimura, T.; Takeuchi, T.; Hori, M. Inhibition of poly(ADP-ribose) glycohydrolase activity by cyclic peptide antibiotics containing piperazic acid residues. *Proc. Jpn. Acad.* 2002, *78*(Ser. B), 15-17.

[40]   Coyle, D. L.; Kim, H.; Jacobson, E. L. ; Jacobson, M. K. Synthesis and characterizaton of potent and selective cell permeable inhibitors of poly(ADP-ribose) glycohydrolase. *Med. Sci.* 2003, *9*(Suppl. 1), 15.

Poly(ADP-ribose) Preparation Using Anion-Exchange Column Chromatography

Takashi Shimokawa, Hideki Ogino, Daisuke Maeda, Hitoshi Nakagama, Takashi Sugimura and Mitsuko Masutani

Biochemistry Division, National Cancer Center Research Institute, 5-1-1, Tsukiji, Chuo-ku, Tokyo 104-0045, Japan.

Abstract: Poly(ADP-ribose) polymerase (PARP) polyADP-ribosylates proteins involved in various physiological processes. Accumulated evidence suggests not only protein-conjugated poly(ADP-ribose) but also protein-free poly(ADP-ribose) function in various physiological processes. There are increasing occasions that require protein-free poly(ADP-ribose) to study the function and dynamics of poly(ADP-ribose) in cells. However, the availability of poly(ADP-ribose) is still limited because a chemical synthesis method has not been established. Here, we describe an improved method for the preparation of protein-free poly(ADP-ribose), synthesized enzymatically by using a recombinant PARP-1 expression system and purified with an anion-exchange column chromatography. This method will be useful for biochemical and biological investigation of poly(ADP-ribose) functions and dynamics.

Keywords: poly(ADP-ribose) polymerase, poly(ADP-ribose), anion-exchange column, preparation

Introduction

Poly(ADP-ribose) is a biomacromolecule produced in a polyADP-ribosylation reaction, one of the post-translational modifications of proteins.[1] The involvement of PARP-1 in development of insulin-dependent diabetes mellitus[2-4] cerebral ischemia[5] and in maintenance of genomic stability[6,7] has been reported. The presence of poly(ADP-ribose) polymerase family proteins[8-10] has been reported and proteins which bind poly(ADP-ribose) have been described.[11-14] Understanding the role of protein-conjugated and released poly(ADP-ribose) molecules has become a more important issue than ever.

Preparation of poly(ADP-ribose) polymer is necessary for studying polyADP-ribosylation and poly(ADP-ribose) metabolism. Unlike DNA or RNA, chemical synthesis of poly(ADP-ribose) is still not practical and enzymatic synthesis of poly(ADP-ribose) is being carried out. Small scale preparation of radioisotopically-labelled or unlabelled poly(ADP-ribose) has been carried out. Using extracts of cultured cells or tissues such as calf thymus, poly(ADP-ribose) synthesis reaction was carried out and after detachement of protein and removal of protein, DNA and RNA, poly(ADP-ribose) was purified with a molecular sieve column, hydroxylapatite column, ion-exchange column or an affinity-column chromatography with boronate resin. Molecular sieve columns such as Zorvax G450 (Dupont) and HPLC column TSK-125 (Bio-Rad) have been used,[15] Boronate resins, such as dihydroxyboryl Bio-Rex 70 (Bio-Rad) have an affinity with cis-diol groups and have been also used for preparation of poly(ADP-ribose). Elution of poly(ADP-ribose) is carried out with diluted HCl.[16] The size fractionation of poly(ADP-ribose) is not possible with boronate resin. Ion-exchange column for HPLC has been applied for purification of oligo- and poly(ADP-ribose).[17] Another frequently used procedure for the purification of poly(ADP-ribose) involves hydroxylapatite column chromatography separation.[18] This step can remove short DNA or RNA fragments. It also allows rough size-dependent elution of poly(ADP-ribose). However, size fractionation of poly(ADP-ribose) cannot be achieved by this procedure. In addition, elution with high concentrations of phosphate buffer requires further exclusive dialysis to remove phosphates.

To improve the purification method of poly(ADP-ribose), we utilized QIAGEN-tip (Qiagen, Hilden, Germany), which is commercially available for plasmid DNA purification.[19] This column contains pre-packed QIAGEN resin, which has a hydrophilic surface coated with diethylaminoethyl groups.

Correspondence: M. Masutani, Biochemistry Division, National Cancer Center Research Institute, 5-1-1, Tsukiji, Chuo-ku, Tokyo, 104-0045, Japan. Tel: +81-3-3542-2511; Ext: 4550; Fax: +81-3-3542-2530; Email: mmasutan@ncc.go.jp.

Poly(ADP-ribose) can be eluted with a buffer containing NaCl, which is easily removed by dialysis. Furthermore, this column allows better size separation of the polymer. This method was only briefly mentioned in our previous reports[20,21] and here we describe the detailed procedure and the characterization of the prepared poly(ADP-ribose). The procedure described here will be useful for researchers who study poly(ADP-ribose) function.

Materials and Methods

Poly(ADP-ribose) was prepared using an *E. coli* crude extract that overexpressed human PARP-1, as described.[22] The *E. coli* crude extract from one liter contained approximately 72 units of PARP activity (one unit of PARP activity was defined as 1 nmol ADP-ribose incorporation per minute at 25 °C). Briefly, pellets of *E. coli* expressing PARP-1 from a 4-liter culture (approximately 10 ml) were suspended in 20 ml of lysis buffer-200 μg/ml lysozyme and incubated at 0 °C for 15 min, then NaCl and NP-40 were added to 0.6 M and 1.0%, respectively. A supernatant was obtained by ultracentrifuge at 39,800 g for 60 min at 4 °C, desalted with Centriprep (Millipore, Billerica, Massachusetts, U.S.A.) and was subjected to poly(ADP-ribose) synthesis reaction. A reaction mixture of 50 ml containing the above lysate, 30 mM MgCl₂, 20 μg/ml histone (Sigma-Aldrich Corp.), 10 μg/ml activated calf thymus DNA (Sigma-Aldrich Corp.), 1 mM NAD, and protein-ase inhibitor cocktail (Complete, Roche Applied Science, Mannheim, Germany) was prepared and incubation was carried out for 60 min at 25 °C. The reaction was stopped by adding 1/50 volume of 5 N NaOH, and further incubated for 60 min at 37 °C to release poly(ADP-ribose) from acceptor proteins.

After addition of Tris-HCl (pH 7.5) to 50 mM, the pH was adjusted to 7.5 with HCl, and incubated overnight after addition of SDS to 0.1% and proteinase K (Merck and Co., Inc., Readington Township, New Jersey, U.S.A.) to 50 μg/ml at 37 °C in a volume of approximately 50 ml. Protein was removed by extracting with equal volumes (50 ml) of water-saturated phenol/chloroform (1:1 (v/v)), mixing vigorously for 10 min, centri-fuging at 1,500 g at room temperature and taking the supernatant. The sample was then extracted with equal volumes of chloroform two times, and the aqueous layer obtained after centrifugation was processed to ethanol precipitation. To the aqueous

layer, 1/10 volume of 3 M sodium acetate (pH 5.0) and 2 volumes of ethanol were added. The sample was kept at −80 °C for 15 min and centrifuged at 10,000 g for 15–20 min at 4 °C and the pellet was taken. After washing the pellet with 30 ml of 70% ethanol and drying, the pellet was resuspended in 20 ml of a buffer consisting of 50 mM Tris-HCl (pH 7.5), 10 mM MgCl₂, 5 mM CaCl₂, 4 μg/ml DNase I (Takara Bio Inc., Otsu, Shiga, Japan), 4 μg/ml RNase A (Sigma-Aldrich Corp.), 10 μg/ml nuclease P1 (Yamasa Corp., Choshi, Chiba, Japan), and 1% toluene and incubated overnight at 37 °C. After addition of pronase E (Sigma-Aldrich Corp.) to 0.1 mg/ml, incubation was continued at 37 °C for 2 hr. Following extraction with equal volumes of water-saturated phenol/chloroform 1:1(v/v) for 10 min by mixing vigorously, as described above, the sample was centrifuged at 1,500 g at room temperature and the supernatant taken. The sample was then extracted with equal volumes of chloroform two times, and the aqueous layer obtained after centrifugation was processed to ethanol precipitation. Poly(ADP-ribose) was recovered from the aqueous layer by ethanol precipitation by adding ammonium acetate (pH 7.0) to 2 M and adding 2.5 volumes of ethanol at room temperature. After centrifugation at 3,000 g for 15 min at 4 °C, washing the pellet with 70% ethanol and drying, the pellet was resuspended into 10 ml of a solution consisting 50 mM Tris-HCl (pH 7.0) and 10 mM EDTA.

A column of QIAGEN-tip 500 was equilibrated with 10 ml of buffer QBT [750 mM NaCl, 50 mM MOPS (pH 7.0), 15% ethanol, 0.15% Triton X-100], and allowed to empty by gravity flow.[19] Ten ml of poly(ADP-ribose) solution was applied to the QIAGEN-tip with gravity flow. After washing with 2 × 10 ml wash buffer [50 mM MOPS (pH 7.0), 0.4 M NaCl, 15% ethanol], stepwise elution of poly(ADP-ribose) was conducted with 10 ml of elution buffer-1 [50 mM MOPS (pH 7.0), 0.6 M NaCl, 15% ethanol], 10 ml of elution buffer-2 [50 mM MOPS (pH 7.0), 0.8 M NaCl, 15% ethanol], 10 ml of buffer QC [50 mM MOPS (pH 7.0), 1.0 M NaCl, 15% ethanol] and 10 ml of buffer QF [50 mM MOPS (pH 7.0), 1.2 M NaCl, 15% ethanol]. Ethanol in each buffer can be substituted with propanol. Washing and elution buffers were degassed or autoclaved to shorten the chromato-graphic steps. Each fraction was analyzed for poly(ADP-ribose) chain length distribution by 20% polyacrylamide gel electrophoresis as described,[23]

and dialyzed against 3 liters of water at room temperature overnight. The desalting step could be replaced by ethanol or isopropanol precipitation. Capillary electrophoresis was performed using ssDNA Gel Linear Polyacrylamide with Tris-borate-7 M urea (P/ACE, Beckman Coulter Inc., Fullerton, California, U.S.A).

For preparation of ^{32}P-labelled-poly(ADP-ribose), an *E. coli* pellet from a 500 ml culture was prepared and 1–3 volumes of lysis buffer [50 mM Tris-HCl (pH 8.0), 1 mM dithiothreitol, 1 mM phenylmethanesulfonyl fluoride, 10 μg/ml leupeptin] were added. Egg white lysozyme was added to 200 μg/ml and incubated at 0 °C for 15 min. After adding NaCl to 0.6 M and NP-40 to 1.0%, centrifuge was carried out for 45 min at 25,000 *g* at 4 °C. The supernatant, approximately 5 ml, was added to a 50 ml reaction mixture containing 50 mM Tris-Cl (pH 7.5), 1 mM dithiothreitol, 30 mM $MgCl_2$, 20 μg/ml histone (Sigma-Aldrich Corp.), 10 μg/ml activated calf thymus DNA (Sigma-Aldrich Corp.), 10–20 μM [adenylate-^{32}P] NAD (0.46 MBq/nmol, NEN, PerkinElmer, Inc., Waltham, Massachusetts, U.S.A.), proteinase inhibitor cocktail (Complete) and incubation was carried out for 60 min at 25 °C. This reaction was stopped with 1/50 volume of 5 N NaOH, and further incubated for 60 min at 37 °C to release poly(ADP-ribose) from acceptor proteins and processed as described above for preparation of cold poly(ADP-ribose). Either QIAGEN-tip 500 or -tip 100 was used for preparation of ^{32}P-poly(ADP-ribose) as described above.

For determination of the size of ^{32}P-poly(ADP-ribose), hydrolysis by purified venom phosphodiesterase was carried out. Phosphodiesterase from *Crotalus adamanteus* (Worthington Biochemical Corp., Lakewood, New Jersey, U.S.A.) was purified by a Blue-Sepharose column to remove any traces of phosphomonoesterase.[24,25] The sample was digested in a reaction mixture containing 10 mM sodium phosphate buffer (pH 7.0), 10 mM $MgCl_2$, and 0.004 unit of the purified phosphodiesterase[24] and incubated for 3 hr or overnight. The samples were spotted on F1440 (Scheleicher and Schuell, Dassel, Germany) TLC plate and developed with solvent A: isobutyric acid/25% NH_4OH/H_2O (50/1.1/28.9 by volume), and B: 0.1 M sodium phosphate (pH 6.8)/ammonium sulfate/n-propanol (100/60/2, v/w/v). The radioactivity of each spot was analyzed by BAS2000 (Fujifilm, Minato-ku, Tokyo, Japan). Each spot was

characterized as AMP, phosphoribosyl-AMP (PR-AMP), diphosphoribosyl-AMP ((PR)$_2$AMP). The average polymer size was calculated as [AMP + PR-AMP + (PR)$_2$AMP]/[AMP − (PR)$_2$AMP] as described.[26]

Results and Discussion

As shown in Figure. 1A, a rapid and size separation of ^{32}P-poly(ADP-ribose) was achieved with the QIAGEN-tip column by changing the pH and salt concentration of the elution buffer. The average polymer size and the average number of branching points were determined by two-dimensional
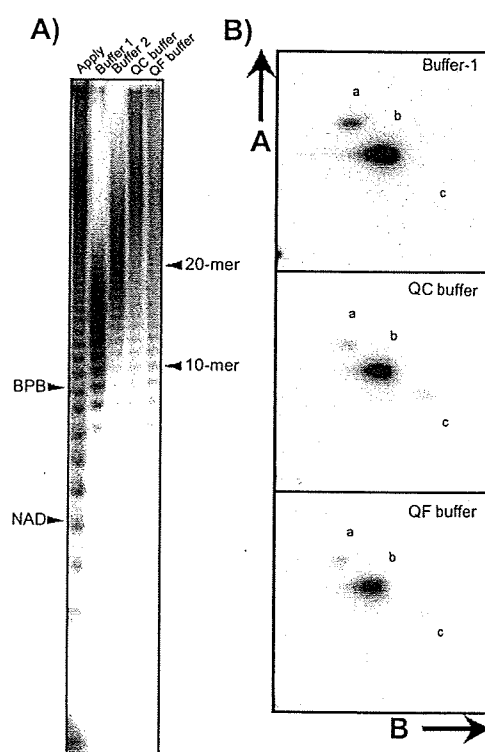

Figure. 1. A) ^{32}P-Poly(ADP-ribose) fraction on QIAGEN-tip. 20% polyacrylamide gel electrophoresis analysis. One μl of samples of each fraction was mixed with 20 μl of sample buffer [50% urea, 25 mM NaCl, 4 mM EDTA, 0.02% xylene cyanol, 0.02% bromophenol blue], and applied to 20% polyacrylamide gel (acrylamide/bisacrylamide, 19.85/0.25 by weight).[23] Applied fraction (apply), eluted fractions with buffer 1, buffer 2, QC buffer and QF buffer were subjected to analysis. The radioactivity of the gel was analyzed by BAS2000. B) Two-dimensional TLC for characterization of ^{32}P-poly(ADP-ribose). After hydrolysis by purified venom phosphodiesterase, the samples (eluent with buffer-1, QC buffer and QF buffer) were spotted on a TLC plate and developed with solvent A and B as described in Materials and Methods. The radioactivity of each spot was analyzed by BAS2000. Each spot was characterized as AMP ((a), phosphoribosyl-AMP (PR-AMP) (b), and diphosphoribosyl-AMP ((PR)$_2$AMP) (c).

thin-layer chromatography after phosphodiesterase treatment[26] as shown in Figure. 1B. The typical yield of cold poly(ADP-ribose) prepared from 4 liters of lysate of the *E. coli* was 0.393 μmol (ADP-ribose residues, 216 μg), 1.419 μmol (780 μg), 0.156 μmol (86 μg) for buffer-1, QC and GF, respectively. Mean chain-length in each fraction was 17-mer, 20-mer, 26-mer, for buffer-1, QC buffer and QF buffer, respectively. Branched poly(ADP-ribose) could be observed in the fractions

eluted with QC and QF. It should be noted that doublet bands were observed as reported by Panzeter et al. due to two different hydrolysis products at the reducing termini.[23] The maximum capacity of QIAGEN-tip 100 and -tip 500 for DNA is around 100 μg and 500 μg, respectively, according to the manufacturer's recommendation. The above result suggests maximum capacity of QIAGEN-tip 500 for poly(ADP-ribose) is approximately 1,000 μg or higher. Figure. 2A shows non-radioisotopic poly(ADP-ribose) prepared using the same method. Figure. 2B shows the capillary electrophoresis pattern of the poly(ADP-ribose). This method should be applicable for rapid and larger scale preparation of poly(ADP-ribose).
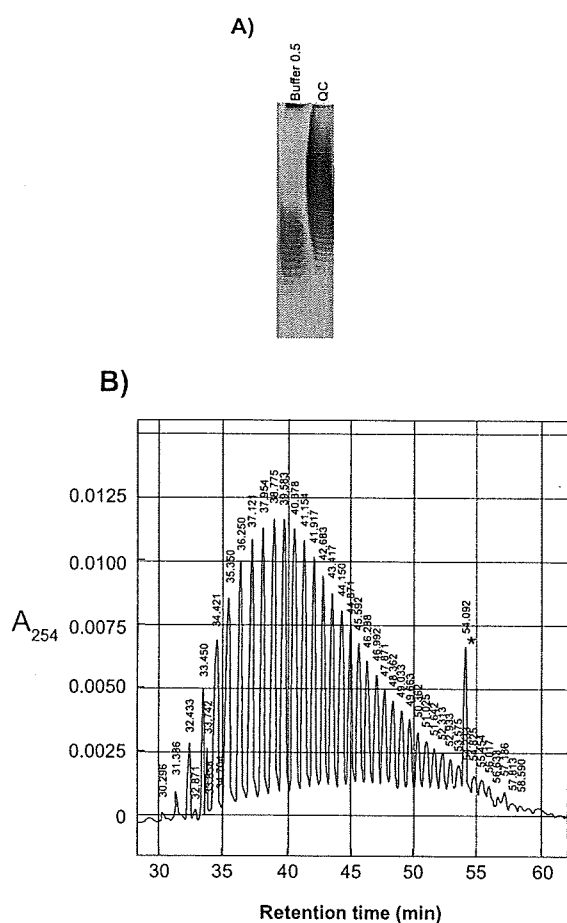
Abbreviations

PARP, poly(ADP-ribose) polymerase; NAD, nicotinamide adenine dinucleotide.

Acknowledgments

Disclosure

The authors report no conflicts of interest.

Figure. 2. A) Analysis of poly(ADP-ribose) by 20% polyacrylamide gel electrophoresis. Twenty μg of buffer 0.5 [50 mM MOPS (pH 7.0), 0.5 M NaCl, 15% propanol] eluted fraction and QC buffer [50 mM MOPS (pH 7.0), 1.0 M NaCl, 15% propanol] eluted fraction were applied. Note that ethanol in the buffers was substituted with propanol. After electrophoresis, the gel was subjected to silver-staining (Daiichi Pure Chemicals Co. Ltd., Chuo-ku, Tokyo, Japan). **B)** Capillary electrophoresis profile of poly(ADP-ribose). The fraction eluted with QC buffer was subjected to capillary electrophoresis. Detection was carried out with measurement of UV absorbance at 254 nm. The retention time of each peak is shown. A peak marked with an asterisk is derived from an unknown UV absorbing substance in the preparation.

References

1. Sugimura T. Poly(adenosine diphosphate ribose). *Prog Nucleic Acid Res Mol Biol.* 1973;13:127–151.
2. Masutani M, Suzuki H, Kamada N, et al. Poly(ADP-ribose) polymerase gene disruption conferred mice resistant to streptozotocin-induced diabetes. *Proc Natl Acad Sci U S A.* 1999;96:2301–2304.
3. Pieper AA, Brat DJ, Krug DK, et al. Poly(ADP-ribose) polymerase-deficient mice are protected from streptozotocin-induced diabetes. *Proc Natl Acad Sci U S A.* 1999;96:3059–3064.
4. Yamamoto H, Okamoto H. Protection by picolinamide, a novel inhibitor of poly(ADP-ribose) synthetase, against both streptozotocin-induced depression of proinsulin synthesis and reduction of NAD content in pancreatic islets. *Biochem Biophys Res Commun.* 1980;95:474–481.
5. Eliasson MJ, Sampei K, Mandir AS, et al. Poly(ADP-ribose) polymerase gene disruption renders mice resistant to cerebral ischemia. *Nat Med.* 1997;3:1089–1095.
6. de Murcia JM, Niedergang C, Trucco C, et al. Requirement of poly(ADP-ribose) polymerase in recovery from DNA damage in mice and in cells. *Proc Natl Acad Sci U S A.* 1997;94:7303–7307.

7. Wang ZQ, Stingl L, Morrison C, et al. PARP is important for genomic stability but dispensable in apoptosis. *Genes Dev.* 1997;11: 2347–2358.

8. Ame JC, Spenlehauer C, de Murcia G. The PARP superfamily. *Bioessays.* 2004;26:882–893.

9. Schreiber V, Dantzer F, Ame JC, de Murcia G. Poly(ADP-ribose): novel functions for an old molecule. *Nat Rev Mol Cell Biol.* 2006;7:517–528.

10. Smith S, Giriat I, Schmitt A, de Lange T. Tankyrase, a poly(ADP-ribose) polymerase at human telomeres. *Science.* 1998;282:1484–1487.

11. Ahel I, Ahel D, Matsusaka T, et al. Poly(ADP-ribose)-binding zinc finger motifs in DNA repair/checkpoint proteins. *Nature.* 2008;451:81–85.

12. Egloff MP, Malet H, Putics A, et al. Structural and functional basis for ADP-ribose and poly(ADP-ribose) binding by viral macro domains. *J Virol.* 2006;80:8493–8502.

13. Nozaki T, Masutani M, Akagawa T, Sugimura T, Esumi H. Non-covalent interaction between poly(ADP-ribose) and cellular proteins: an application of a poly(ADP-ribose)-western blotting method to detect poly(ADP-ribose) binding on protein-blotted filter. *Biochem Biophys Res Commun.* 1994;198:45–51.

14. Pleschke JM, Kleczkowska HE, Strohm M, Althaus FR. Poly(ADP-ribose) binds to specific domains in DNA damage checkpoint proteins. *J Biol Chem.* 2000;275:40974–40980.

15. Brochu G, Duchaine C, Thibeault L, Lagueux J, Shah GM, Poirier GG. Mode of action of poly(ADP-ribose) glycohydrolase. *Biochim Biophys Acta.* 1994;1219:342–350.

16. Jacobson MK, Payne DM, Alvarez-Gonzalez R, Juarez-Salinas H, Sims JL, Jacobson EL. Determination of in vivo levels of polymeric and monomeric ADP-ribose by fluorescence methods. *Methods Enzymol.* 1984;106:483–494.

17. Hakam A, McLick J, Kun E. Separation of poly(ADP-ribose) by high-performance liquid chromatography. *J Chromatogr.* 1984;296: 369–377.

18. Miwa M, Sugimura T. Structure of poly(ADP-ribose). *Methods Enzymol.* 1984;106:441–450.

19. Budelier K, Schorr J. Purification of DNA by anion-exchange chromatography. *Curr Protoc Mol Biol.* 2001;Chapter 2, Unit2 1B.

20. Shimokawa T, Masutani M, Nagasawa, et al. Isolation and cloning of rat poly(ADP-ribose) glycohydrolase: presence of a potential nuclear export signal conserved in mammalian orthologs. *J Biochem.* 1999;126:748–755.

21. Shirato M, Tozawa S, Maeda D, Watanabe M, Nakagama H, Masutani M. Poly(etheno ADP-ribose) blocks poly(ADP-ribose) glycohydrolase activity. *Biochem Biophys Res Commun.* 2007;355: 451–456.

22. Ikejima M, Noguchi S, Yamashita R, Suzuki H, Sugimura T, Miwa M. Expression of human poly(ADP-ribose) polymerase with DNA-dependent enzymatic activity in Escherichia coli. *Biochem Biophys Res Commun.* 1989;163:739–745.

23. Panzeter PL, Althaus FR. High resolution size analysis of ADP-ribose polymers using modified DNA sequencing gels. *Nucleic Acids Res.* 1990;18:2194.

24. Ikejima M, Marsischky G, Gill DM. Direction of elongation of poly(ADP-ribose) chains. Addition of residues at the polymerase-proximal terminus. *J Biol Chem.* 1987;262:17641–17650.

25. Oka J, Ueda K, Hayaishi O. Snake venom phosphodiesterase: simple purification with Blue Sepharose and its application to poly(ADP-ribose) study. *Biochem Biophys Res Commun.* 1978;80:841–848.

26. Keith G, Desgres J, de Murcia G. Use of two-dimensional thin-layer chromatography for the components study of poly(adenosine diphosphate ribose). *Anal Biochem.* 1990;191:309–313.

Analysis of poly(ADP-ribose) polymerase-1 (*PARP1*) gene alteration in human germ cell tumor cell lines

Hideki Ogino[a,b], Robert Nakayama[c], Hiromi Sakamoto[c], Teruhiko Yoshida[c], Takashi Sugimura[a], Mitsuko Masutani[a,b,*]

[a]*Biochemistry Division, National Cancer Center Research Institute, 1-1 Tsukiji 5-chome, Chuo-ku, Tokyo 104-0045, Japan*
[b]*ADP-ribosylation in Oncology Project, National Cancer Center Research Institute, 1-1 Tsukiji 5-chome, Chuo-ku, Tokyo 104-0045, Japan*
[c]*Genetics Division, National Cancer Center Research Institute, 1-1 Tsukiji 5-chome, Chuo-ku, Tokyo 104-0045, Japan*

Abstract   The poly(ADP-ribose) polymerase-1 protein (PARP-1) functions in DNA repair, maintenance of genomic stability, induction of cell death, and transcriptional regulation. We previously analyzed alterations of the *PARP1* gene in 16 specimens of human germ cell tumors, and found a heterozygous sequence alteration that causes the amino acid substitution Met129Thr (M129T) in both tumor and normal tissues in a single patient. In this study, aberration of the *PARP1* gene and protein was further analyzed in human germ cell tumor cell lines. We found a nonheterozygous sequence alteration that causes the amino acid substitution Glu251Lys (E251K) located at a conserved peptide stretch of PARP-1 in cell line NEC8. Sequencing of 95 samples from Japanese healthy volunteers revealed that all the samples were homozygous for the wild-type alleles at M129T and E251K. The M129T allele is thus suggested to be a rare single-nucleotide polymorphism (SNP). We observed a decrease in auto-poly(ADP-ribosyl)ation activity of PARP-1 proteins harboring M129T or E251K amino acid substitution, but the difference was not statistically significant. The levels of PARP-1 and poly(ADP-ribosyl)ation were heterogeneous among germ cell tumor cell lines. The SNPs of the *PARP1* gene, as well as differences in the levels of PARP-1 and poly(ADP-ribosyl)ation of proteins, may influence germ cell tumor development and responses to chemotherapy and radiotherapy. © 2010 Elsevier Inc. All rights reserved.

1. Introduction

Poly(ADP-ribose) polymerase-1 (PARP-1) is activated by DNA damage and catalyzes poly(ADP-ribosyl)ation of various proteins, including PARP-1 itself, using nicotinamide adenine dinucleotide (NAD$^+$) as a substrate. PARP-1 is involved in DNA repair, maintenance of genomic stability, and cell death induction. We and others have previously reported that *Parp-1* knockout (*Parp-1$^{-/-}$*) mice showed higher susceptibility to carcinogenesis induced by alkylating agents in the colon [1] and lung [2], compared with wild-type (*Parp-1$^{+/+}$*) mice. The incidence of spontaneous tumors developed at an advanced age in the liver was also higher in *Parp-1$^{-/-}$* mice [3,4].

Involvement of PARP-1 in the development of human cancer has not yet been fully clarified. In human cancers,

increased expression of the *PARP1* gene has been reported in Ewing's sarcoma [5,6], in malignant lymphoma [7], and in the familial adenomatous polyposis (FAP) tumors [8]. Decreased expression of the *PARP1* gene has been observed in several gastric and colon cancer cell lines [6], grade II and III endometrial carcinomas [9], and in some breast cancers [10].

The A/A homozygotes of the V762A single-nucleotide polymorphism (SNP) in the *PARP1* gene have been reported to be associated with decreased activity of PARP-1. The A/A homozygotes are shown to be associated with an increased risk for prostate cancer in European-origin subjects [11] and in lung cancer and esophageal cancers in Chinese heavy smokers [12,13]. In the case of lung and esophageal cancers, a twofold increase in risk with the A/A homozygotes was observed in Chinese smokers [12,13]. The combination of the 762A allele of the *PARP1* gene and the 399 G allele of the *XRCC1* gene was associated with increased risk of lung, esophageal, and gastric cardia cancers [12–15].

---

* Corresponding author. Tel.: +81-3-3542-2511; fax: +81-3-2542-2530.

E-mail address: mmasutan@ncc.go.jp (M. Masutani).

PARP-1 also participates in the transcriptional regulation of some genes [16–18] and in cellular differentiation [18–20]. *Parp-1$^{-/-}$* mouse embryonic stem cells show preferential induction of the trophoblast lineage [20], including trophoblast giant cells (TGCs), during teratocarcinoma formation in vivo or during cell culture in vitro [19]. The biochemical properties of TGCs resemble those of syncytiotrophoblastic giant cells (STGCs) of human germ cell tumors [21,22]. It is thus suggested that *PARP1* deficiency may possibly trigger differentiation to STGCs during germ cell tumor formation. The appearance of STGCs in trophoblastic or choriocarcinomatous human . germ cell tumors has been reported to be associated with poor prognosis [21]. Teratocarcinoma cells undergo differentiation into epithelial cells in vitro, at least in part, in the presence of the PARP inhibitor 3-aminobenzamide [23].

The aberrations of the *PARP1* gene in 16 human germ cell tumors were previously analyzed, and a heterozygous sequence alteration (A<u>T</u>G to A<u>C</u>G) that causes amino acid substitution, Met129Thr (M129T) [24] was found in one patient in both cancer and normal tissues. In the present study, we further analyzed aberration of the *PARP1* gene and poly(ADP-ribosyl)ation level in human germ cell tumor cell lines and evaluated effects of any amino acid alterations found on PARP-1 function.

2. Materials and methods

2.1. Cell culture

Cell lines JEG-3, NCCIT, PA-1, Tera-1, and Tera-2 were purchased from the American Type Culture Collection (ATCC, Manassas, VA). Cell lines ITOII and NEC8 were purchased from the Japanese Collection of Research Bioresources (http://cellbank.nibio.go.jp/cellbank_e.html). Cell lines NEC14 and NEC15 were purchased from the Riken Bioresource Center (http://www.brc.riken.go.jp/inf/en/index.shtml). Each cell line was cultured under the conditions recommended by the providers. The growing cells at mid-late log phase were used as the materials for preparation of genomic DNA, total RNA, and total protein.

For transfection experiments, an immortalized *Parp-1$^{-/-}$* mouse embryonic fibroblast (MEF) clone, PH13b, established from spontaneously immortalized *Parp-1$^{-/-}$* MEFs [25] was used. The cells were cultured at 37°C under 5% CO_2 and 95% humidity.

2.2. Direct sequencing of the human PARP1 gene

Polymerase chain reaction (PCR)-based direct sequencing of all 23 exons of the *PARP1* gene in germ cell tumor cell lines was performed as previously described [24]. Oligonucleotide primer sets for the 23 exons were designed from intron sequences of each exon as previously described [24]. Amplified PCR products were subjected to sequence analysis (ABI PRISM 310 genetic analyzer,

Applied Biosystems, Carlsbad, CA; model CEQ8000, Beckman Coulter, Fullerton, CA). Sequence comparison was performed against the sequence of the human *PARP1* gene (NCBI accession numbers NT_004559 and NT_167186) and its cDNA (NCBI accession numbers M18112, M32721, M17081, J03473, BC037545, and BC014206).

2.3. Pyrosequencing

Pyrosequencing for codon 129 and codon 251 of the *PARP1* gene was performed as previously described [26]. Briefly, genomic DNA samples were extracted from blood of 95 healthy Japanese volunteers, and samples were subjected to genotyping by pyrosequencing using the PSQ96 System (Pyrosequencing, Uppsala, Sweden). For sequencing of codons 129 and 251, we used 5′-CGTGCAAGGGGTGTA-3′ and 5′-TGAACACACTTTCTTTAGC-3′ as sequencing primers, respectively. In the case of codon 251, the sequencing result of one sample was not informative.

All subjects provided informed consent, and the study was approved by the Ethical Committee of the National Cancer Center of Japan.

2.4. Construction of PARP1 mutants

PARP1 mutant cDNA harboring either M129T, E251K, or K940R amino acid substitution was prepared using primers harboring respective mutation and Phusion polymerase (Fynnzymes, Espoo, Finland) according to the protocol of the QuikChange site-directed mutagenesis kit (Stratagene, La Jolla, CA). The human *PARP1* cDNA [27] was modified using PCR to harbor restriction enzyme recognition sites of *Sal*I, *Sma*I, *Age*I, and *Xba*I at the 5′ and 3′ terminus, respectively, and modified Kozack's sequences derived from pEGFP-C1 (Clontech Laboratories, Mountain View, CA) in the 5′-UTR (untranslated region) of the *PARP1* cDNA. The *PARP1* cDNA harboring either M129T, E251K, and K940R amino acid substitution was inserted into pcDNA3.1(+)hygro (Invitrogen, Carlsbad, CA) for measurement of PARP-1 enzymatic activity. pEGFP-C1 was used for construction of the GFP protein fused to the N-terminus of PARP-1 protein for analysis of subcellular localization.

2.5. Transfection of the PARP1 mutant constructs

Four micrograms of each construct was transfected into the *Parp-1$^{-/-}$* MEFs in six-well plates using Lipofectamine 2000 (Invitrogen). At 24 hours after transfection, whole-cell extracts were prepared by suspending cells in a lysis solution containing 50 mmol/L Tris–HCl (pH 6.8), 10% glycerol, 2% sodium dodecyl sulfate (SDS), complete protease inhibitor cocktail tablets (Roche Applied Science, Mannheim, Germany), and 10% β-mercaptoethanol. The samples were frozen in liquid nitrogen and stored at −80°C until use.

2.6. Activity gel analysis

PARP-1 enzymatic activity was measured as auto-poly(ADP-ribosyl)ation activity of PARP-1, as described elsewhere [28]. Briefly, crude extracts were separated by 6% SDS—polyacrylamide gel electrophoresis (SDS-PAGE) containing 100 μg/mL of sonicated salmon sperm DNA as an activated DNA. After renaturation of proteins in the gel, the gel was incubated in a reaction mixture containing 50 mmol/L Tris—HCl (pH 8.0), 1 mmol/L dithiothreitol, 50 μmol/L [^{32}P]adenylate-labeled nicotinamide adenine dinucleotide (1 μCi/mL, NEN—PerkinElmer, Waltham, MA), and 25 mmol/L MgCl$_2$ at 37°C for 1 hour. The gel was fixed with 10% methanol—30% acetic acid (v/v) solution, and washed with 5% trichloroacetic acid—0.2% sodium pyrophosphate. The radioactivies of the dried gels were analyzed using a BAS-2500 bio-imaging analyzer (Fujifilm, Tokyo, Japan).

2.7. Western blot analysis

Whole-cell extracts were prepared by suspending cells in a lysis solution containing 50 mmol/L Tris-HCl (pH 6.8), 10% glycerol, 2% SDS, complete protease inhibitor cocktail tablets (Roche Applied Science), and 10% β-mercaptoethanol, followed by sonication. Equivalent protein amounts of lysate (8 μg) were separated by 4—20% gradient SDS-PAGE. After transfer of proteins to Immobilon-P polyvinylidene difluoride membranes (Millipore, Billerica, MA), the membrane was incubated with anti-poly(ADP-ribose) monoclonal antibody 10H (Alexis Biochemicals—Enzo Life Sciences, Lausanne, Switzerland) [29], anti-PARP-1 monoclonal antibody C2-10 (Oncogene Research Products, Merck Chemicals, Darmstadt, Germany), F1-23 (Alexis Biochemicals) or anti-α-tubulin monoclonal antibody DM1A (MP Biomedicals, Irvine, CA). Immune complexes were visualized using a horseradish peroxidase-linked secondary antibody and an enhanced chemiluminescence reaction ECL kit (Amersham Biosciences, Piscataway, NJ). The PARP-1 protein level was quantified using a LAS-3000 bio-imaging analyzer (Fujifilm).

3. Results

3.1. Sequence alterations in germ cell tumor cell lines

The human germ cell tumor cell lines used in this study are listed in Table 1. All 23 exons and their flanking regions of the *PARP1* gene in nine germ cell tumor cell lines were sequenced. Sequence alterations and SNPs found in the *PARP1* gene are listed in Table 2. We found that the two missense SNPs, Phe54Leu (F54L) and V762A, were described in the NCBI (National Center for Biotechnology Information) database of SNPs. These SNPs of F54L and V762A in NEC14 and NEC15 were observed as nonheterozygous sequence alterations. A nonheterozygous sequence

Table 1
Human germ cell tumor cell lines used in this study

Cell line	Type	Reference
NEC8	Embryonal carcinoma: testis	Motoyama et al., 1987 [39]
NEC14	Embryonal carcinoma, choriocarcinoma: testis	Motoyama et al., 1987 [39]
NEC15	Embryonal carcinoma, yolk sac tumor: testis	Motoyama et al., 1987 [39]
ITOII	Embryonal carcinoma: testis	Motoyama et al., 1987 [39]
Tera-1	Embryonal carcinoma: lung	Fogh et al., 1978 [40]
Tera-2	Embryonal carcinoma: lung	Fogh et al., 1978 [40]
NCCIT	Embryonal carcinoma	Teshima et al., 1988 [41]
PA-1	Teratoma: ovary	Zeuthen et al., 1980 [42]
JEG-3	Choriocarcinoma: placenta	Kohler et al., 1971 [43]

alteration (<u>G</u>AG to <u>A</u>AG) that causes amino acid substitution Glu251Lys (E251K) in NEC8 was also found (Table 2 and Fig. 1). This sequence alteration has not been listed in the NCBI database of SNPs. Further information for NEC8 was not available, and it is not known whether this is a somatic or germ line mutation or sequence alteration caused during establishment of this cell line.

To determine whether E251K is a common SNP in the Japanese population, we sequenced 94 samples from Japanese healthy volunteers using a pyrosequencing method. Similarly, sequencing data were obtained from 95 volunteers for M129T, which we previously found in a germinoma and its normal tissue from a patient [24]. In both cases, all the sequenced samples were homozygous: <u>G</u>AG (251E) and A<u>T</u>G (129M). None were heterozygous, which suggests that the two amino acid substitutions, E251K and M129T, are not common SNPs in the Japanese population.

Three synonymous SNPs were also found at Asp81, Ala284, and Lys352 (Table 2). In the noncoding region, a SNP of G to C in 5′-UTR, 17 bases upstream of the translation initiation site, downstream of a putative ETS-1-binding site (base −26 to −22) [30]), was found (rs907187). NEC15 had a nonheterozygous C allele, and ITOII and Tera-1 had heterozygous G/C alleles. We also noted that the nonheterozygous allele at a SNP in intron 2 (rs1805405) was observed at higher frequency (3/9) than a heterozygous allele (1/9) in germ cell tumor cell lines, but the difference was not statistically significant. NEC8, NEC15, and ITOII had the nonheterozygous A allele, whereas NCCIT had heterozygous C/A alleles.

3.2. Effect of amino acid alteration on the activity of PARP-1

The effect of amino acid substitution of methionine to threonine at codon 129 (Met129Thr) and glutamic acid to lysine at codon 251 (Glu251Lys) on PARP-1 enzymatic activity was examined. We transiently expressed the mutated PARP-1 harboring either M129T or E251K substitution in the *Parp-1*$^{-/-}$ MEFs, and measured the enzymatic activity of PARP-1 by the activity gel method. Both *Parp-1* mutants showed a decrease in PARP-1 activity relative to the wild type, although the difference was not

Table 2

Sequence alterations and SNPs found in the *PARP1* gene in human germ cell tumor cell lines

	Exon	Nucleotide[a]	No.	Germ cell tumor cell line[b]	SNP ID[c]	Heterozygosity[c]
				Amino acid substitution		
Phe54Leu	2	TT**C**	8	NEC8, NEC14, ITOII, Tera-1, Tera-2, NCCIT, PA-1, JEG-3	rs3738708	0.023
		TTC/TT**G**	0			
		TT**G**	1	NEC15		
Glu251Lys	6	**G**AG	8	NEC14, NEC15, ITOII, Tera-1, Tera-2, NCCIT, PA-1, JEG-3	not listed	not listed
		GAG/**A**AG	0			
		AAG	1	NEC8		
Val762Ala	17	G**T**G	7	NEC8, ITOII, Tera-1, Tera-2, NCCIT, PA-1, JEG-3	rs1136410	0.351
		G**T**G/G**C**G	0			
		G**C**G	2	NEC14, NEC15		
				SNPs without amino acid substitution		
Asp81Asp	2	GA**C**	5	NEC8, Tera-2, NCCIT, PA-1, JEG-3	rs1805404	0.372
		GA**C**/GA**T**	2	ITOII, Tera-1		
		GA**T**	2	NEC14, NEC15		
Ala284Ala	7	GC**T**	5	NEC15, ITOII, Tera-2, PA-1, JEG-3	rs1805414	0.498
		GC**T**/GC**C**	2	NCCIT, Tera-1		
		GC**C**	2	NEC8, NEC14		
Lys352Lys	8	AA**A**	8	NEC14, NEC15, ITOII, Tera-1, Tera-2, NCCIT, PA-1, JEG-3	rs1805415	0.379
		AA**A**/AA**G**	0			
		AA**G**	1	NEC8		
				SNPs in noncoding region		
5'-UTR (−17 bp)		G	6	NEC8, NEC14, Tera-2, NCCIT, PA-1, JEG-3	rs907187	0.357
		G/C	2	ITOII, Tera-1		
		C	1	NEC15		
Intron 2 (5592 bp)		C	5	NEC14, Tera-1, Tera-2, PA-1, JEG-3	rs1805405	0.362
		C/A	1	NCCIT		
		A	3	NEC8, NEC15, ITOII		

Abbreviations: SNP, single nucleotide polymorphism; UTR, untranslated region.

[a] The altered nucleotide is indicated by underscoring.

[b] See Table 1 for cell lines.

[c] SNP identifiers and average estimated heterozygosity data are from the NCBI database of SNPs, available at http://www.ncbi.nlm.nih.gov/SNP/index.html.

statistically significant ($P = 0.1266$ for 129T, $P = 0.2752$ for 251K) (Fig. 2A).

Cellular localization of E251K and M129T mutants was also analyzed as GFP-fusion protein expressed in the $Parp$-$1^{-/-}$ MEF. The cellular localization of another *PARP1* mutant harboring K940R amino acid substitution was analyzed as well [24]. Wild-type, 129T, 251K, and
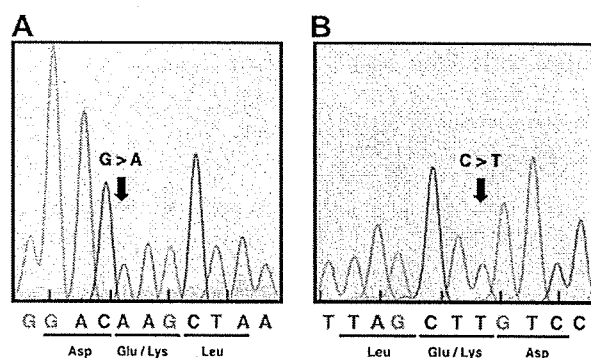

Fig. 1. Electropherograms of sequences surrounding codon 251 of the *PARP1* gene in NEC8 cells. Sequence alterations of both strands were confirmed by sequencing using the sense (A) and anti-sense (B) primers.

940R protein localized exclusively in the nuclei (Fig. 2B). The localization is observed in a punctuated manner in the nuclei, and the localization pattern did not differ between wild-type and the mutants.

3.3. Levels of PARP-1 protein, activity, and poly(ADP-ribosyl)ation

The levels of PARP-1 proteins were measured by Western blot analysis (Fig. 3). PA-1 and NEC8 cells both showed lower levels of PARP-1 proteins. We also examined the enzymatic activity of PARP-1 as PARP-1 auto-poly(ADP-ribosyl)ation activity using whole-cell extracts (Fig. 3, activity gel analysis). PA-1 and NEC8 cells both showed lower levels of auto-poly(ADP-ribosyl)ation activity, compared with the other cell lines analyzed. PA-1, NEC8, and also Tera-2 exhibited lower levels of overall poly(ADP-ribosyl)ation of proteins, compared with the other cell lines.

4. Discussion

Among the germ cell tumor cell lines analyzed in this study, five cell lines were established in Japan, and these
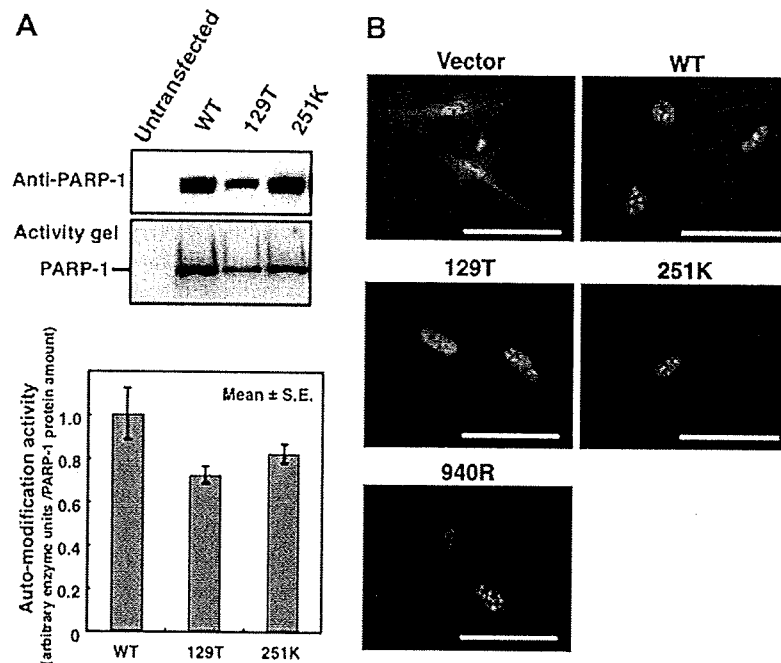
Fig. 2. Effects of amino acid alteration in PARP-1 on enzymatic activity and subcellular localization. (A) Semiquantitative analysis of auto-poly(ADP-ribosyl)ation activity of wild-type and mutant PARP-1 proteins in the whole cell extracts from the *Parp-1$^{-/-}$* mouse embryonic fibroblasts transfected with either the wild-type (WT) or mutant PARP-1 expression plasmid. The representative result of the activity gel analysis (middle panel) and Western blot analysis of PARP-1 (top panel) is shown. The auto-poly(ADP-ribosyl)ation activity normalized to the expressed PARP-1 level measured by Western blot analysis. A linear relationship between the amount of PARP-1 and auto-poly(ADP-ribosyl)ation activity was confirmed (data not shown). (B) Subcellular localization of GFP-fused PARP-1. At 24 hours after transfection, localization of wild-type PARP-1 and mutant proteins harboring either 129T, 251K, or 940R amino acid substitution was observed exclusively in the nuclei. Scale bars: 10 μm.

may reflect a spectrum of polymorphisms in the Japanese population. We found a nonheterozygous sequence alteration (GAG to AAG) that causes amino acid substitution of E251K of PARP-1 in NEC8. Because the corresponding normal tissue samples were not available for the NEC8 cell line, we could not examine whether E251K is a SNP. It is not known whether the nonheterozygosity represents a homozygosity or an allelic loss, nor could we exclude the possibility that this sequence alteration was introduced during or after establishment of NEC8. We previously reported that a heterozygous sequence alteration that causes amino acid alteration of M129T was observed in a human germ cell tumor specimen [24]. Our analysis in the present study suggests that the sequence alterations of E251K and M129T are not common SNPs in the Japanese population.

E251K is located at a peptide stretch conserved among species in the C-terminus of a DNA binding domain close to the nuclear localization signal. The third zinc-binding motif (codon 295–321) [28,31] is present close to codon 251. The third zinc-binding domain of codon 216–366 is required for dimerization of PARP-1. K249E substitution is reported to decrease PARP-1 enzymatic activity [32]. A decrease in auto-poly(ADP-ribosyl)ation activity but no alteration in nuclear localization of PARP-1 harboring M129T or E251K amino acid substitution was observed; however, we noted that NEC8, which has a nonheterozyous

E251K allele, had a lower level of PARP-1 protein in the extract (Fig. 3). The effects on DNA binding or DNA repair regulation, as well as stability, should be further analyzed.

Within nine cell lines, both nonheterozygous minor alleles of V762A and intron 2 (5,592 bp) (SNP ID, rs1805405) showed a tendency of higher frequencies than expected, although it was not statistically significant. These tendencies are similar to the result obtained with our previous study using 16 germ cell tumor specimens [24]. The V762A SNP was found to be associated with the risk of prostate cancers in European-origin subjects, in whom the A/A genotype showed a twofold increase in susceptibility [11]. Recently the *PARP1* V762A polymorphism has been reported to reduce the enzymatic activity of PARP-1 and the ability of interaction with *XRCC1* [15,33]; however, a decrease in PARP-1 auto-poly(ADP-ribosyl)ation activity and overall poly(ADP-ribosyl)ation levels was not observed in NEC14, which harbors a nonheterozygous V762A allele (Table 2 and Fig. 3).

The nonheterozygous allele of SNP rs1805405, located within the polypyrimidine tract close to the 3′ splice acceptor site in the intron 2, was observed at a higher frequency (3/9) than expected, as in the case with human germ cell tumor specimens (3/16) [24]. A stretch of (C/T)6NCAGG(C/T) at a splicing acceptor site is relatively conserved in the introns [34]. The polypyrimidine tract is
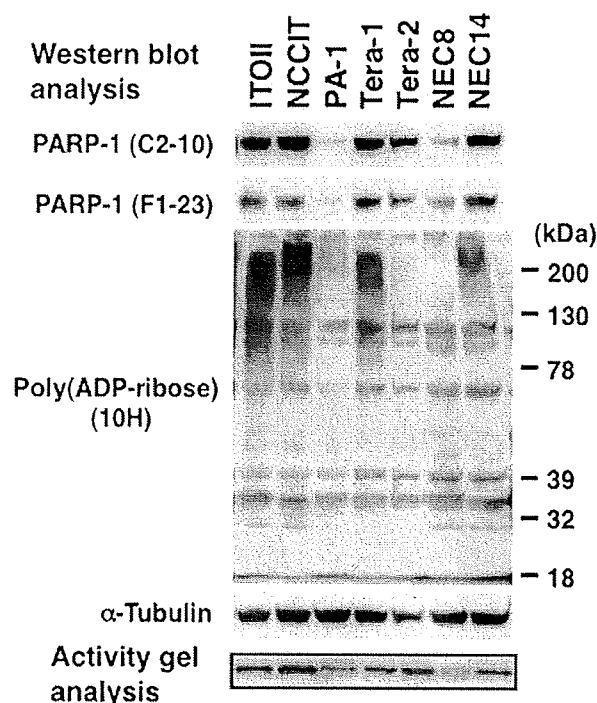
Fig. 3. PARP-1 protein levels and activity, with overall poly(ADP-ribosyl)-ation protein levels. Western blot analysis was performed for detection of PARP-1 protein and poly(ADP-ribosyl)ated proteins (upper and middle panels). For detection of PARP-1 enzymatic activity, activity gel analysis was performed (bottom panel) to analyze PARP-1 auto-poly(ADP-ribosyl)-ation activity; 30 μg of cell extracts was subjected to 6% SDS-PAGE in the presence of activated DNA in the gel.

highly conserved, and the frequency of adenine at this position is low (~7%) [35]. In the case of all introns of *PARP1* reference sequences (NCBI numbers NT_004559 and NT_167186), the frequency of adenine at this position is ~9%. In the case of hereditary nonpolyposis colorectal cancer proband, a single base-pair T-to-A transversion at position −11 of the *MLH1* gene intron 1 splice acceptor site caused exon 2 skipping [36]. We detected only a full-length transcript of *PARP1* in the cell lines harboring minor alleles of the SNP at intron 2 by Northern blot analysis (data not shown). Whether the SNP at intron 2 of *PARP1* affects the splicing efficiency of exon 3 needs further investigation.

It is noteworthy that the poly(ADP-ribosyl)ation level is lower in NEC8, PA-1, and Tera-2, compared with other germ cell tumor cell lines. The lower poly(ADP-ribosyl)a-tion level in NEC8 and PA-1 could be explained by the lower PARP-1 level, but that is not the case for Tera-2. Ac-tivites of other PARP family proteins or of PARG, a major poly(ADP-ribose) degradation enzyme, may also affect the poly(ADP-ribosyl)ation level in Tera-2. We did not find any SNPs or other base alterations in the 3′UTR of the *PARP1* gene in nine cell lines. Therefore, the mechanism for lower levels of PARP-1 in NEC8 and PA-1 may not be due to altered posttranscriptional regulation of PARP-1.

In this study, we identified sequence alterations, including SNPs, in the *PARP1* gene of human germ cell tumor cell lines. The nonheterozygous minor alleles of SNPs at V762A and intron 2 showed a slightly higher frequency. Differences in the levels of PARP-1 and poly(ADP-ribosyl)a-tion were observed. Because poly(ADP-ribosyl)ation reac-tion is involved in several physiological processes in cancer cells, including DNA repair and differentiation, the alteration of PARP-1 activity may affect the development of cancers through multiple processes. It is also suggested that PARP family proteins, including PARP-2, may complement PARP-1 functions [37]. It may therefore be necessary to examine aberrations of PARP-1 and other PARP family proteins in cancers not only at gene expression levels but also at protein or enzymatic activity levels. Clinical trials are ongoing with PARP inhibitors in combination with chemo-therapeutic agents [38]. Understanding the mechanisms of functional regulation of PARP-1 in cancer cells is important. Because the activity of PARP-1 and other PARP family members is important in DNA repair and cell death induc-tion, the levels of PARP-1 and poly(ADP-ribosyl)ation activity may also substantially affect the outcome of cancer therapies that target DNA.

References

[1] Nozaki T, Fujihara H, Watanabe M, Tsutsumi M, Nakamoto K, Kusuoka O, Kamada N, Suzuki H, Nakagama H, Sugimura T, Masutani M. Parp-1 deficiency implicated in colon and liver tumori-genesis induced by azoxymethane. Cancer Sci 2003;94:497–500.

[2] Tsutsumi M, Masutani M, Nozaki T, Kusuoka O, Tsujiuchi T, Nakagama H, Suzuki H, Konishi Y, Sugimura T. Increased suscepti-bility of poly(ADP-ribose) polymerase-1 knockout mice to nitrosa-mine carcinogenicity. Carcinogenesis 2001;22:1–3.

[3] Tong WM, Cortes U, Hande MP, Ohgaki H, Cavalli LR, Lansdorp PM, Haddad BR, Wang ZQ. Synergistic role of Ku80 and poly(ADP-ribose) polymerase in suppressing chromosomal aber-rations and liver cancer formation. Cancer Res 2002;62:6990–6.

[4] Masutani M, Nakagama H, Sugimura T. Poly(ADP-ribosyl)ation in relation to cancer and autoimmune disease. Cell Mol Life Sci 2005;62:769–83.

[5] Prasad SC, Thraves PJ, Bhatia KG, Smulson ME, Dritschilo A. Enhanced poly(adenosine diphosphate ribose) polymerase activity and gene expression in Ewing's sarcoma cells. Cancer Res 1990; 50:38–43.

[6] Masutani M, Nozaki T, Sasaki H, Yamada T, Kohno T, Shimizu K, Gotoh M, Shiraishi M, Yokota J, Hirohashi S, Nakagama H, Sugimura T. Poly(ADP-ribose) polymerase-1 gene in human tumor

cell lines: its expression and structural alteration. Proc Jpn Acad Ser B Phys Biol Sci 2004;80B:114—8.

[7] Menegazzi M, Scarpa A, Carcereri de Prati A, Menestrina F, Suzuki H. Correlation of poly(ADP-ribose)polymerase and p53 expression levels in high-grade lymphomas. Mol Carcinog 1999; 25:256—61.

[8] Idogawa M, Yamada T, Honda K, Sato S, Imai K, Hirohashi S. Poly(ADP-ribose) polymerase-1 is a component of the oncogenic T-cell factor-4/β-catenin complex. Gastroenterology 2005;128: 1919—36.

[9] Ghabreau L, Roux JP, Frappart PO, Mathevet P, Patricot LM, Mokni M, Korbi S, Wang ZQ, Tong WM, Frappart L. Poly(ADP-ribose) poly-merase-1, a novel partner of progesterone receptors in endometrial cancer and its precursors. Int J Cancer 2004;109:317—21.

[10] Bièche I, de Murcia G, Lidereau R. Poly(ADP-ribose) polymerase gene expression status and genomic instability in human breast cancer. Clin Cancer Res 1996;2:1163—7.

[11] Lockett KL, Hall MC, Xu J, Zheng SL, Berwick M, Chuang SC, Clark PE, Cramer SD, Lohman K, Hu JJ. The ADPRT V762A genetic variant contributes to prostate cancer susceptibility and deficient enzyme function. Cancer Res 2004;64:6344—8.

[12] Zhang X, Miao X, Liang G, Hao B, Wang Y, Tan W, Li Y, Guo Y, He F, Wei Q, Lin D. Polymorphisms in DNA base excision repair genes ADPRT and XRCC1 and risk of lung cancer. Cancer Res 2005;65:722—6.

[13] Hao B, Wang H, Zhou K, Li Y, Chen X, Zhou G, Zhu Y, Miao X, Tan W, Wei Q, Lin D, He F. Identification of genetic variants in base excision repair pathway and their associations with risk of esophageal squamous cell carcinoma. Cancer Res 2004;64:4378—84.

[14] Zhang Z, Miao XP, Tan W, Guo YL, Zhang XM, Lin DX. Correlation of genetic polymorphisms in DNA repair genes ADPRT and XRCC1 to risk of gastric cancer [In Chinese]. Ai Zheng 2006;25:7—10.

[15] Miao X, Zhang X, Zhang L, Guo Y, Hao B, Tan W, He F, Lin D. Adenosine diphosphate ribosyl transferase and x-ray repair cross-complementing 1 polymorphisms in gastric cardia cancer. Gastroen-terology 2006;131:420—7.

[16] Ogino H, Nozaki T, Gunji A, Maeda M, Suzuki H, Ohta T, Murakami Y, Nakagama H, Sugimura T, Masutani M. Loss of Parp-1 affects gene expression profile in a genome-wide manner in ES cells and liver cells. BMC Genomics 2007;8:41.

[17] Krishnakumar R, Gamble MJ, Frizzell KM, Berrocal JG, Kininis M, Kraus WL. Reciprocal binding of PARP-1 and histone H1 at promoters specifies transcriptional outcomes. Science 2008;319: 819—21.

[18] Quenet D, Gasser V, Fouillen L, Cammas F, Sanglier-Cianferani S, Losson R, Dantzer F. The histone subcode: poly(ADP-ribose) poly-merase-1 (Parp-1) and Parp-2 control cell differentiation by regu-lating the transcriptional intermediary factor TIF1β and the heterochromatin protein HP1α. FASEB J 2008;22:3853—65.

[19] Nozaki T, Masutani M, Watanabe M, Ochiya T, Hasegawa F, Nakagama H, Suzuki H, Sugimura T. Syncytiotrophoblastic giant cells in teratocarcinoma-like tumors derived from Parp-disrupted mouse embryonic stem cells. Proc Natl Acad Sci USA 1999;96: 13345—50.

[20] Hemberger M, Nozaki T, Winterhager E, Yamamoto H, Nakagama H, Kamada N, Suzuki H, Ohta T, Ohki M, Masutani M, Cross JC. Parp1-deficiency induces differentiation of ES cells into trophoblast deriva-tives. Dev Biol 2003;257:371—81.

[21] von Hochstetter AR, Sigg C, Saremaslani P, Hedinger C. The significance of giant cells in human testicular seminomas: a clini-co-pathological study. Virchows Arch A Pathol Anat Histopathol 1985;407:309—22.

[22] Masutani M, Nozaki T, Watanabe M, Ochiya T, Hasegawa F, Nakagama H, Suzuki H, Sugimura T. Involvement of poly(ADP-ribose) polymerase in trophoblastic cell differentiation during tumorigenesis. Mutat Res 2001;477:111—7.

[23] Ohashi Y, Ueda K, Hayaishi O, Ikai K, Niwa O. Induction of murine teratocarcinoma cell differentiation by suppression of poly(ADP-ribose) synthesis. Proc Natl Acad Sci USA 1984;81: 7132—6.

[24] Shiokawa M, Masutani M, Fujihara H, Ueki K, Nishikawa R, Sugimura T, Kubo H, Nakagama H. Genetic alteration of poly(ADP-ribose) polymerase-1 in human germ cell tumors. Jpn J Clin Oncol 2005;35:97—102.

[25] Nozaki T, Fujihara H, Kamada N, Ueda O, Takato T, Nakagama H, Sugimura T, Suzuki H, Masutani M. Hyperploidy of embryonic fibro-blasts derived from Parp-1 knockout mouse. Proc Jpn Acad Ser B Phys Biol Sci 2001;77:121—4.

[26] Nakayama R, Sato Y, Masutani M, Ogino H, Nakatani F, Chuman H, Beppu Y, Morioka H, Yabe H, Hirose H, Sugimura H, Sakamoto H, Ohta T, Toyama Y, Yoshida T, Kawai A. Association of a missense single nucleotide polymorphism, Cys1367Arg of the WRN gene, with the risk of bone and soft tissue sarcomas in Japan. Cancer Sci 2008; 99:333—9.

[27] Uchida K, Morita T, Sato T, Ogura T, Yamashita R, Noguchi S, Suzuki H, Nyunoya H, Miwa M, Sugimura T. Nucleotide sequence of a full-length cDNA for human fibroblast poly(ADP-ribose) poly-merase. Biochem Biophys Res Commun 1987;148:617—22.

[28] Masutani M, Nozaki T, Hitomi Y, Ikejima M, Nagasaki K, de Prati AC, Kurata S, Natori S, Sugimura T, Esumi H. Cloning and functional expression of poly(ADP-ribose) polymerase cDNA from Sarcophaga peregrina. Eur J Biochem 1994;220:607—14.

[29] Kawamitsu H, Hoshino H, Okada H, Miwa M, Momoi H, Sugimura T. Monoclonal antibodies to poly(adenosine diphosphate ribose) recognize different structures. Biochemistry 1984;23: 3771—7.

[30] Soldatenkov VA, Albor A, Patel BK, Dreszer R, Dritschilo A, Notario V. Regulation of the human poly(ADP-ribose) polymerase promoter by the ETS transcription factor. Oncogene 1999;18: 3954—62.

[31] Langelier MF, Servent KM, Rogers EE, Pascal JM. A third zinc-binding domain of human poly(ADP-ribose) polymerase-1 coordi-nates DNA-dependent enzyme activation [Erratum in: J Biol Chem 2008;283:22884]. J Biol Chem 2008;283:4105—14.

[32] Trucco C, Flatter E, Fribourg S, de Murcia G, Ménissier-de Murcia J. Mutations in the amino-terminal domain of the human poly(ADP-ribose) polymerase that affect its catalytic activity but not its DNA binding capacity. FEBS Lett 1996;399:313—6.

[33] Wang XG, Wang ZQ, Tong WM, Shen Y. PARP1 Val762Ala poly-morphism reduces enzymatic activity. Biochem Biophys Res Com-mun 2007;354:122—6.

[34] Nakata K, Kanehisa M, DeLisi C. Prediction of splice junctions in mRNA sequences. Nucleic Acids Res 1985;13:5327—40.

[35] Stephens RM, Schneider TD. Features of spliceosome evolution and function inferred from an analysis of the information at human splice sites. J Mol Biol 1992;228:1124—36.

[36] Clarke LA, Veiga I, Isidro G, Jordan P, Ramos JS, Castedo S, Boavida MG. Pathological exon skipping in an HNPCC proband with MLH1 splice acceptor site mutation. Genes Chromosomes Cancer 2000;29:367—70.

[37] Miwa M, Masutani M. PolyADP-ribosylation and cancer. Cancer Sci 2007;98:1528—35.

[38] Ratnam K, Low JA. Current development of clinical inhibitors of poly(ADP-ribose) polymerase in oncology. Clin Cancer Res 2007; 13:1383—8.

[39] Motoyama T, Watanabe H, Yamamoto T, Sekiguchi M. Human testic-ular germ cell tumors in vitro and in athymic nude mice. Acta Pathol Jpn 1987;37:431—48.

[40] Fogh J. Cultivation, characterization, and identification of human tumor cells with emphasis on kidney, testis, and bladder tumors. Natl Cancer Inst Monogr 1978;49:5—9.